Timing of the Miocene-Quaternary magmatic intrusions in the Tanga offshore basin: correlation to age equivalent deposits in the Eyasi-Wembere basin and their implications for petroleum potential

BENATUS NORBERT MVILE (benimvile@yahoo.com)
The University of Dodoma https://orcid.org/0000-0002-5883-4281
Emily Barnabas Kiswaka
University of Dar es Salaam College of Natural and Applied Sciences
Olawale Olakunle Osinowo
University of Ibadan Faculty of Science
Isaac Muneji Marobhe
University of Dar es Salaam College of Natural and Applied Sciences
Abel Idowu Olayinka
University of Ibadan Faculty of Science
Elisante Elisaimon Mshiu
University of Dar es Salaam College of Natural and Applied Sciences

Research Article

Keywords: Tanga offshore basin, magmatic intrusions, Eyasi-Wembere, core logging, elemental proxies

Posted Date: March 16th, 2022

DOI: https://doi.org/10.21203/rs.3.rs-1208836/v1

Abstract

Detailed 2D qualitative seismic interpretation, coupled with core logging and analysis of elemental proxies, has been used to assess petroleum potential of the Miocene-Quaternary successions of the Tanga offshore basin. These successions have been intruded by magmatic sills and dykes. Based on seismic well tie and correlation with age equivalent onshore successions in the Eyasi-Wembere basin, the timing of these intrusions are linked to periods of tectonic episodes that influenced development of the East African Rift basins. Seismic interpretation has shown that these tectonic episodes occurred during the Miocene-Pliocene, Pleistocene and Holocene periods. The magmatic bodies are thought to have promoted source rock maturation and facilitate formation of structural elements for petroleum trapping in the basin.

1. Introduction

Tanga basin is located in the northeastern Tanzania with both onshore and offshore compartments. This work is focused on the offshore compartment (located in an area between Zanzibar and Pemba and the Indian Ocean shoreline, Fig. 1) where seismic data for subsurface mapping was available. The deposition of the study area was influenced by the EARs. The EARs has been associated with massive volcanism since its beginning (Boccaletti et al., 1999; Franke et al., 2015). However, there is no report of the existence of magmatic intrusions in the Miocene-Quaternary stratigraphy of the study area, thus, limited petroleum exploration has been undertaken.

The aim of this work therefore, was to assess the petroleum potential of the Miocene-Quaternary section of the study area, which may be impacted by magmatic activities. Magmatic intrusions may be major components of a petroleum system if source rock maturation, structural development and formation of fractured reservoirs are taken into consideration (Spacapan et al., 2020). These are the reasons behind investigation for possible presence of similar magmatic products that have been found in other age equivalent rift basins an example of which is the Eyasi-Wembere basin. The tectonic history of the Eyasi-Wembere basin is closely linked to development of the Miocene-Quaternary interval in the Tanga offshore basin. The Eyasi-Wembere basin is located at the southwestern end of the eastern branch of the EARs, just to the south of the Serengeti Plain (Ebinger et al., 1997; Foster et al., 1997; Mbede, 2001; Fig. 1).

In this work, a detailed 2D seismic interpretation has been used to assess the petroleum potential of the study area based on presence of magmatic bodies and other petroleum system elements. Correlation has been made to age equivalent deposits that have been cored in the Eyasi-Wembere basin whose tectonic history is closely linked to development of the Miocene-Quaternary interval in the Tanga offshore basin.

2. Geologic Setting

2.1. Tectonic development

Formation of the Tanga Basin resulted from multiple extensional tectonic regimes (Kapilima, 2003). These extensional regimes include the Permo-Triassic, Jurassic-Cretaceous and the Cenozoic tectonic events (Kent et al., 1971; Kapilima, 2003). The Cenozoic tectonic event led to development of the East African Rift sysem (Kent et al., 1971; Kapilima, 2003). The East African Rift system (EARs) was formally subdivided into eastern and western onshore branches (e.g. Ebinger et al., 1997; Foster et al., 1997) but recent studies have reported a third component, the offshore branch of EARs (e.g. Franke et al., 2015) which is evident in the Tanga offshore basin (Mvile et al., 2021). Both onshore and offshore compartments of the sedimentary basins that their development were partly influenced by the EARs have been dissected by more or less near vertical faults (Ebinger et al., 1997; Foster et al., 1997, Mbede, 2001; Franke et al., 2015; Mvile et al., 2021).

2.2 Regional structural settings: correlation to Eyasi-Wembere basin

The East African Rift (EAR) system is characterized by narrow elongate zones of thinned continental lithosphere linked with asthenospheric intrusions in the upper mantle (Chorowicz, 2005). The system encompasses vast expanse of land, with several valleys and basins, stretching for about 6000 km in a more or less N-S trend (Chorowicz, 2005). The basins, and associated sub-basins, are bounded by major normal faults and are separated by tilted blocks (Chorowicz, 2005). The EAR system has two main branches, the eastern and western branches (Ebinger et al., 1997; Foster et al., 1997; Chorowicz, 2005). A southeastern branch, in the Mozambique Channel, is considered to be the third offshore branch of the EAR system (Chorowicz, 2005; Franke et al., 2015). The western branch extends for about 2100 km from Lake Albert and ends in the Lake Nyasa basin in the south (Chorowicz, 2005).The eastern branch extends for about 2200 km from the Afar triangle to the north through the Ethiopian rift, Turkana lows, the Kenyan rifts, and ends in the northern Tanzanian basins to the south (Chorowicz, 2005). The eastern branch has three arms namely the Eyasi-Wembere, Natron-Manyara-Barangida and Pangani rifts. The offshore branch is characterized by more or less N-S trending sub-basins that are about 25 km wide (Fig. 2; Mvile et al., 2021). Here correlation is made between sedimentary successions in the offshore branch of the EARs within the Tanga Basin and the Eyasi-Wembere basin, a south-eastern arm of the eastern branch of the EARs for a better understanding of the Miocene-Quaternary successions of the Tanga offshore basin. The Eyasi-Wembere basin has been chosen for correlation purpose because of the presence of cores (Wembere 1-3 whose locations are shown in Fig. 1) that have penetrated deposits which are age equivalent to the studied interval in the Tanga offshore basin.

3. Dataset And Methodology

Three techniques have been used to accomplish this work. These are 2D seismic interpretation, core logging and analysis of elemental proxies.

3.1. Seismic interpretation

2D seismic interpretation has been used to identify seismic intervals containing remnant tectonic features and suggest presence of magmatic bodies within the Miocene-Quaternary stratigraphy of the Tanga offshore basin. These features were then correlated with similar features in the age equivalent deposits of the Eyasi-Wembere basin, a component in the eastern branch of the East African Rift System for confirmation of timing of magmatic activity relative to basin development. Age assignment to the studied seismic sections in the Tanga offshore basin was done through a seismic-well tie shown on Fig. 3. Further seismic work involved assessment of potential source, reservoirs and cap rocks intervals for better understanding of the petroleum system of the area.

3.1.1. Identification of tectonic features on seismic

Different basin fill geometries are used to indicate different sedimentation episodes relative to fault movement during active tectonics and intervening periods of tectonic quiescence. A total fill geometry characterized by a wedge shape with internal strata expanding toward the bounding fault has been widely used to reflect syn-rift sedimentation (Nøttvedt et al., 1995; Ravnås & Bondevik, 1997; Ravnås & Steel, 1998; Elliott et al., 2017; Kiswaka & Felix, 2020). A wedge shaped fill geometry characterized by internal strata with uniform thickness has been used to indicate post rift infill of remnant rift topography (e.g. Müller et al., 2005). The syn-rift successions are interpreted to imply deposition during active tectonics at a time when sedimentation was keeping pace with fault movement/basin subsidence (Nøttvedt et al., 1995; Ravnås & Bondevik, 1997; Ravnås & Steel, 1998; Elliott et al., 2017; Kiswaka & Felix, 2020). The Pre rift and post rift deposits are interpreted to have been emplaced before and after active tectonics respectively (e.g. Prosser, 1993). Similar interpretation techniques have been used in this work to identify timing of tectonics episodes. Identification of the tectonic episodes was based on subsurface mapping of pre rift, syn-rift and post rift deposits due to their characteristic seismic expressions. The identified tectonic episodes were then linked to occurrence of magmatic/volcanic deposits in the Tanga offshore basin stratigraphy whereby correlation is made to age equivalent intervals in the Eyasi-Wembere basin.

3.1.2. Identification of magmatic bodies on seismic

Several workers have reported presence of magmatic features in different basins due to their manifestations on seismic images. Examples of these features include igneous sills and dykes, hydrothermal vents and intrusion-related forced folds (e.g. Trude, 2004; Hanset et al., 2008; Zhao et al., 2014; Zhao et al., 2016; Eide et al., 2018). Magmatic deposits may be identified on seismic based on stratal termination patterns, presence of eye shaped features and localized folds, and localized high amplitude discordant seismic reflections within sedimentary basin fills (e.g. Hanset et al., 2008; Zhao et al., 2014; Zhao et al., 2016). Similar interpretation techniques have been adopted herein to characterize Miocene-Quaternary stratigraphy of the Tanga offshore basin.

3.2. Core logging

The Eyasi-Wembere cores (whose locations are shown on Fig.s 1 & 4) were logged to identify intervals containing volcanic products and establish stratigraphy of the Eyasi-Wembere basin for correlation to age equivalent deposits in the Tanga offshore basin. Ages of the successions penetrated by the Wembere cores were determined based on biostratigraphy data reported on Table 1.

3.3. Elemental proxies

A total of 845 elemental measurements were collected on the Wembere-3 core and plotted against depth for qualitative analysis of elemental distributions in the Eyasi-Wembere basin. The elemental distributions analysis was aimed at constraining intervals that contain volcanic products in the Eyasi-Wembere stratigraphy and identify igneous origin and compositions of the associated magmas. The igneous origins and compositions of the associated magmas are key to understanding whether the volcanic products were delivered from external sources (e.g. Ngorongoro volcanic centers whose locations are shown on Fig. 4) or were produced by volcanism that occurred contemporaneously with the rifting. Correlation to Tanga offshore basin will then help to understand origin and timing of emplacement of the suggested magmatic bodies (see section 3.1) in the study area.

3.3.1. Measurement of element values

Element values were recorded by using a portable X-Ray Fluorescence (pXRF) scanner. The pXRF scanner is a quick and non-destructive tool for characterizing elemental distributions across stratigraphic intervals of interest. The diameter of measurement for this tool is around 0.5 cm, therefore uncertain results may occur in intervals with coarse grains. The scanning interval was inconsistent (10-20 cm) because of the observed lithological changes/uniformity on the measured core. Thirty-one different elements were measured by the pXRF from Wembere-3 core. These elements are: V, As, Ti, Cr, Mn, Fe, Co, Ni, Cu, Zn, Sr, Zr, Mo, W, Ca, P, S, Cl, K, Se, Rb, Y, Ag, Cd, Sn, Sb, Hg, Pb, Bi, Th and U. Only few of these elements have been used in this work because (1) many elements were not present in quantities that could be measured throughout the core, and (2) not all measured elements can be used as proxies for sources of sediments deposited in a basin.

3.3.2. Uses of elemental proxies in sedimentary studies

Elemental proxies have been widely studied to characterize sedimentary systems. The majority of the studies involved determination of depositional conditions of black shales (e.g. Calvert & Pedersen, 1993; Dymond & Collier, 1996; Algeo & Maynard, 2004; Brumsack, 2006; Tribovillard et al., 2006; Schoepfer et al., 2015), establishment of depositional processes of gravity flow deposits where by changes in elemental values were linked to changes in grain size and gravity flow pulses (Friis et al., 2007; Poulsen et al., 2007) and geochemical characterization of erupted magmas that influenced chemical properties of the volcaniclastic deposits (e.g. Pearce & Norry, 1979; Hiscott & Gill, 1992). In the current study, elemental proxies have been used to constrain sedimentary intervals that contain volcanic products within the Miocene-Quaternary stratigraphy of the Eyasi-Wembere basin, suggest igneous origin of the associated

magma, and indicate influence of different sources of sediments into the basin for correlation with age equivalent deposits in the Tanga offshore basin.

Table 1
Biostratigraphy information for selected intervals in the Wembere cores

Depth (m)	Lithological descriptions	Biostratigraphy information
0-10.43	Very fine-coarse lime sandstone. Occasional quartz grains are seen	Presence of Ostracod *Limnocythere* sp suggest late Pleistocene to Holocene age.
10.43-28.82	Fine to medium grained lime sandstone with floating carbonate fragments and occasional spherical carbonate pellets that resemble microfossils. Very fine quartz grains and volcanic tuffs are also seen in this interval	Poor ostracods population density and fossilized remains of calcified filamentous/tubular and egg-like features. The The *Limnocythere* species indicates the late Pleistocene to Holocene age while the egg-like features indicate cyanobacterial/algal origin.
29.93-32.59	Very fine-coarse lime sandstone with rough texture. Abundant fine quartz grains are seen	Devoid of ostracods but dominated by fossilized tubular filamentous structures and ooids.
37.17-37.26	Loosely compacted, very fine-fine sandstone. Volcanic tuff are common	Devoid of dateable fossils
82.66-83.70	Angular to sub-angular, poor to moderate sorted, fine to coarse grained quartz sandstone.	Devoid of dateable fossils
109.21-109.29m	Poor to moderate sorted, angular to sub-angular, very fine-coarse sandstone	Devoid of dateable fossils
133.75-164.8	Volcanclastic successions containing grain and matrix supported lapillistone and ash tuff intervals. These intervals contain highly consolidated and moderate consolidated sections with occasional very coarse to pebbly lapilli tuff intervals. Quartz grains are also common	Devoid of dateable fossils
169.54 – 170.11	Alternating fine-coarse meta-conglomeratic sandstone marking the basal part of the cored stratigraphy	Devoid of dateable fossils

4. Results And Interpretation

4.1. Ages of the analyzed successions

Ages of the studied successions were established based on seismic well tie (Fig. 3) and bio-stratigraphic dating information accessed from Tanzania Petroleum Development Corporation (Table 1).

4.1.1. Seismic well tie

A seismic well tie was done to assign ages to key horizons in the Tanga offshore basin (Fig. 3). Ages of other seismic intervals were assigned tentatively based on their stratigraphic positions relative to the key markers. The Ras Machuisi North 1 well, retrieved from the Tanga offshore basin located to the west of Zanzibar Island (Fig. 1), was used to accomplish the seismic well tie.

4.1.2. Age constrain from biostratigraphy data

Biostratigraphy data has indicated the late Pleistocene-Holocene age for the upper part of the sedimentary successions penetrated by the Wembere-3 core based on the presence of *Limnocythere* sp ostracods (see biostratigraphy information in Table 1). Similar age indicators have been observed for the sedimentary successions penetrated by Wembere-1 core which was drilled to a total depth of 370 m (TPDC biostratigraphy report). This is because Wembere-3 core was drilled in the southwestern margin of the Eyasi-Wembere sub-basins while Wembere-1 core was drilled in the deeper part of the sub-basin (see Fig. 4 for their relative positions within the basin).

4.2. Established chronostratigraphic schemes

There is no formal chronostratigraphic schemes for the Eyasi-Wembere and Tanga basins. Here the Miocene-Quaternary correlated chronostratigraphic schemes for the Eyasi-Wembere and offshore Tanga basins (Fig. 5) are established based on core logging, seismic interpretation and the accessed literature and core reports. These chronostratigraphic schemes show vertical variations in rock units that are similar to rock distributions in other rift basins with comparable tectonic-magmatic and structural evolution (e.g. Sakai et al., 2013; Ragon et al., 2019).

4.2.1. Stratigraphy of the Eyasi-Wembere basin: core logging

The Eyasi-Wembere stratigraphy is established based on sedimentary logging of Wembere-1 and Wembere-3 cores. In this work, the Wembere cores were logged just for correlation purpose, further detailed sedimentological logging on these cores will be published in the subsequent studies. Based on these cores, the basal part of the Eyasi-Wembere stratigraphy contains weakly metamorphosed, polymictic breccio-conglomerates (Fig. 6A). Clasts of the conglomerates are composed of reddish-brown to light orange colored fragments that were delivered from a well-rounded, medium-conglomeratic sandstone. Complex folding are present in some of the sandstone clasts making up the lower part of the stratigraphy (Fig. 6B). This interval was followed by deposition of volcaniclastic deposits of variable volumes of volcanic lapilli (Fig. 6C) and ashes (Fig. 6D) that is overlain by successions of fining upward beds characterized by poorly sorted, very coarse-conglomeratic sandstone deposits at their basal parts (Fig. 7A & B). Quartz and feldspar grains are common in this interval (Fig. 7A). Upper part of the Eyasi-Wembere stratigraphy contain volcaniclastic deposits dominated by volcanic ashes and coarse-fine grained clastic deposits. Limestone clasts are common in the lower section of the uppermost part of the

stratigraphy (Fig. 8A).The clastic deposits include unconsolidated, coarse sandstone deposits alternating with sandy-mudstone caped by grey-dark grey, red-reddish brown carbonaceous silty-sandy mudstone (Fig. 8B-D).

The weakly metamorphosed, polymictic breccio-conglomerates in the lower part of the Eyasi-Wembere stratigraphy reflect early-rift basin sedimentation (e.g. Sakai et al., 2013) while complex folding is interpreted to be convolute lamination indicating rapid sedimentation and squeezing of wet sediments during deposition of the source beds through which the sandstone fragments were delivered from. Grain size variations displayed by sedimentary successions in the rift basins are mostly linked to water-level change and structural position within the basin (Scholz et al., 1990; Sakai et al., 2013). Similar interpretation is adopted herein to explain observed vertical grain size changes in the Eyasi-Wembere cores (Fig.s 7 & 8). Color differences displayed by the deposits in Fig.s 8 suggest varied depositional oxygen conditions, whereby greyish-reddish dark grey-black deposits are interpreted to have been deposited under oxic and anoxic conditions respectively.

4.2.2. Stratigraphy of the Tanga offshore basin

The Miocene-Quaternary stratigraphy of the Tanga offshore basin is established based on Ras Machuisi North 1 wellbore report, seismic interpretation (see section 4.3 for the results), previous works on the Tanzania coastal basin (e.g. Kapilima, 2003), and field observation, whereby carbonates deposits were observed (e.g. Fig. 9). The Tanga offshore basin experienced continental sedimentation during Miocene-Pliocene period. The Miocene-Pliocene successions are dominated by reddish-brown and minor greenish silty-shale alternating with fine-very coarse quartzose-feldspatic sandstone layers. The Miocene successions of the Tanga offshore basin are barren of dateable fossils just like the Miocene successions of the Eyasi-Wembere basin. Upper part of the basin contain Neogene-Holocene shallow marine clastic sediments and Paleogene-Neogene limestone deposits (e.g. Fig. 9). These clastic sediments are characterized by fine-coarse sand bodies alternating with greenish-grey silty-sandy clays. Seismic features interpreted to represent magmatic bodies (Section 4.3.2) are seen in the Miocene-Quaternary stratigraphy of the Tanga offshore basin.

4.3. Seismic interpretation results

4.3.1. Miocene-Quaternary tectonic features

The studied seismic interval contain wedge shaped sedimentary packages that are expanding toward the bounding faults (Fig. 10). These wedges, characterized by internal strata that are also expanding toward the bounding faults, they first occur just below the Quaternary reflector (Fig. 10). The immediate sedimentary deposits above the Quaternary reflector do not display wedge shaped geometry but they underlie wedge shaped packages with similar features to the wedges below the Quaternary reflector. That is, the observed sedimentary wedges overlie and underlie sedimentary successions characterized by more or less uniform thickness strata (Fig. 10). This sequence repeats itself whereby wedge shaped deposits are seen further up in the stratigraphy of the area (Fig. 10). Based on previous researches from different

basins (e.g. Kiswaka & Felix, 2020), the observed sedimentary wedges are interpreted to mark periods of active tectonics, and therefore syn-rift deposits in the Miocene-Holocene stratigraphy of the Tanga offshore basin. Similarly, the sedimentary packages overlying and underlying the wedges are interpreted to mark intervening periods of tectonic quiescence and are named post rift deposits. The syn-rift deposits below the Quaternary reflector (Fig. 10) are assigned the Miocene-Pliocene tentative age while the Pleistocene and Holocene tentative ages are given to the two syn-rift intervals above the Quaternary reflector due to their stratigraphic positions relative to the Quaternary reflector, but also due to regional reports on rift occurrence in East Africa (See Mollel & Swisher, 2012; Courgeon et al., 2018; Mvile et al., 2021).

4.3.1.1. Faults movement: timing of tectonic pulses

The Quaternary surface map shows that the Miocene-Quaternary development of the Tanga offshore basin has been mostly influenced by the EARs which culminated at the development of about 25 km wide sub-basins with a more or less N-S to NE-SW orientation (e.g. Fig. 2; Mvile et al., 2021). Seismic interpretation revealed that the sea bottom has been dissected by several faults that have been active during different periods to recent time. An example of the timing differences in fault activity is shown by the faults marked 1-3 (Fig. 10). Due to presence of wedge shaped deposits separated by uniform thickness sedimentary packages, periods of active extensional tectonics have been separated from the intervening periods of tectonic quiescence that record post rift sedimentation (Fig. 10). These depositional geometries show that movements on faults 1 and 2 occurred simultaneously since they are both bounding age equivalent syn-rift deposits. However, movement on fault 3 occurred after movements on faults 1 and 2 have stopped. That is sedimentary packages characterized by syn-rift wedges relative to fault 1 pass out to post rift deposits relative to faults 1 and 2, and vice versa. These observation indicate occurrence of localized tectonic pulses along the East African Rift System and that there might be more pulses than what has been reported by previous workers. The fact that all of these faults have dissected the sea bottom despite being active in different times suggests that periodic reactivation and consequently faults movement occurred to recent times. The EARs component studied herein is characterized by two distinct fault system: (1) the dominant N-S to NNE-SSW trending major faults which define key orientations and mark the margins of the Quaternary fault bounded sub-basins in the study area, and (2) the more or less E-W trending faults that mark the northern and southern limits of the Quaternary sub-basins (e.g. Fig. 2).

4.3.2. Miocene-Quaternary magmatic features

Seismic profiles into the Tanga offshore basin contain eye-shaped features in some intervals of the studied stratigraphy. The eye-shaped structures have produced localized folds through which high amplitude reflectors are onlapping onto them (Fig.s 11 & 12). The high amplitude reflectors onlapping onto the localized folds are overlain by intervals characterized by weak near parallel seismic reflectors that are laterally continuous (Fig. 11). In some places, these eye-shaped structures occur adjacent to high amplitude discordant reflectors in the Quaternary stratigraphy (Fig. 12). In this work, the eye shaped

features are found in the upper part of an interval assigned the Miocene-Pliocene tentative age but also in the Quaternary successions (Fig. 12). Another interesting feature was observed on seismic line TA-08-118 (Fig. 12) whereby an inclined linear feature crosscuts the Pliocene-Pleistocene successions without a noticeable displacement. The concurrent occurrence of eye-shaped features and concordant anomalous reflectors are used to confirm presence of magmatic intrusions in the basin. This interpretation is based on previous works that identified magmatic bodies on seismic images from different places (e.g. Trude, 2004; Hanset et al., 2008; Zhao et al., 2014; Zhao et al., 2016; Eide et al., 2018). Following the presence of eye-shaped features and discordant reflectors indicative of magmatic intrusions, the linear feature crosscutting the Pliocene-Holocene successions (Fig. 12) is interpreted to mark igneous dyke in the basin suggesting a relative much younger volcanic activity which is believed to have occurred during the Holocene. The high amplitude reflectors onlapping onto the localized folds are indicative of coarse grained sediments while interval with weak reflections suggest homogeneous shale-very fine sand deposits due to limited contrast in acoustic impedance (e.g. Armitage et al., 2012; Berlin, 2014). One would link the observed features to salt intrusions/ diapirism but this interpretation is less likely due to absence of salt deposits in the Tanga Basin.

4.3.3. Conformity of tectonic features and magmatic bodies

Stratigraphically, the sedimentary wedges on Fig. 10 conform to intervals with linear features crosscutting other sedimentary layers without noticeable displacement (Fig. 12) and areas containing eye shaped features, localized folds and localized high amplitude discordant seismic reflections (Fig.s 11 & 12). That is, occurrence of the observed magmatic elements coincide to periods of tectonic episodes. This observation suggests simultaneous occurrence of the two.

4.4. Elemental distributions and their link to Eyasi-Wembere basin stratigraphy

Elemental distributions have allowed subdivision of the Wembere-3 core into three major zones marked 1, 2 and 3 in Fig.s 13-17. These zones were marked based on distribution trends that are grouped into four. Basal part of the core begins with relatively high Fe and Fe/Ti (group 1) and Zn and Ti (group 2) values that conform to relatively low Rb/Ti and K/Ti (group 3) values (Fig.s 13-16). The group 3 values display a general upward increasing trend in zone 1 until high values are reached in zone 2 and extend to zone 3 where uniform distribution for these values is attained (Fig.s 13-16). The groups 1 and 2 values exhibit a general upward decreasing trend in zone 1, until more or less, uniform distributed low values are reached at about 115 m core depth where zone 2 begins (Fig.s 13-15). Zone 2 extends to around 40 m core depth where a general upward increasing trend (for group 1) and more or less uniform distributed high values (for group 2) characterizing zone 3 begins. Group 4 (Zr and Zr/Ti) values (Fig.s 13 & 17) display similar distribution trends to Fe, Fe/Ti, Zn and Ti (groups 1 & 2) in zones 1 and 2 except that they show a general upward decreasing trend in zone 3. Despite the observed general trends in zones 1-3, these zones are characterized by several peaks and troughs reflecting local influences in elemental distributions.

Basal part of zone 1 (Fig.s 13-17) conform to oldest interval penetrated by Wembere-3 core. The interval is dominated by conglomeratic sandstone that has been slightly metamorphosed. The conglomeratic clasts are characterized by chemically weathered fine-coarse sandstone fragments, some of which have syn-depositional deformation structures (e.g. Fig. 6A & B) reflecting rapid sedimentation during deposition of the source material. An interval overlying this conglomeratic unit, which display upward decreasing trend for groups 1, 2 & 4 values and upward increasing trend for group 4 values, conform to volcaniclastic successions with variable amounts of grain and matrix supported lappilistone and volcanic ashes (e.g. Fig.s 6 C).

Zone 2, which is marked by minimum-uniform distributed groups 1, 3 and 4 values and Maximum-uniform distributed group 3 values, coincide to sedimentary successions dominated by fining upward beds that contain poorly sorted, very coarse-conglomeratic sandstone deposits at their basal parts (Fig. 7).

Zone 3, which shows upward increasing trend for group 1 values, uniform distribution for groups 2 and 3 values and upward decreasing trend for group 4 values, correspond to sedimentary successions characterized by volcanic tuff, lime sandstone and fining upward clastic deposits (Table 1 & Fig. 8).

Several workers have used elemental ratios to reconstruct provenance areas for clastic deposits whereby a decrease in K/Al and Rb/Al ratios have been used to indicate reduced influence in river inputs (e.g. Wehausen & Brumsack, 1999; Martinez-Ruiz et al., 2003; Sangiorgi et al., 2006; Martinez-Ruiz et al., 2015). Here Al was not measured by the pXRF and that is why Ti was used for calculations of elemental ratios. Both Al and Ti have been interpreted to be of detrital origin (Tribovillard et al., 2006), and thus similar interpretation for elemental ratios is assumed in this work. Generally, zone 1 has high values of Fe, Ti, Zn, Fe/Ti and Zr that correspond to low values of K/Ti and Rb/Ti implying dominance of inputs that were not delivered by rivers into the basin. Core logging has shown that zone 1 is dominated by volcanic products. Overall low, uniform distributed Fe, Ti, Zn, Fe/Ti, Zr and Zr/Ti values, which coincide to high, uniform distributed K/Ti and Rb/Ti values in zone 2 indicate dominance of river inputs into the basin as it is reflected by successions of fining upward beds. Influence of volcanic inputs into the basin, during deposition of zone 3, is reflected by an increase in Zn, Fe and Ti values and decrease in Zr and Zr/Ti values (Fig.s 13, 15 & 17). The fact tha K/Ti and Rb/Ti values of zone 3 (Fig. 16) are more or less similar to that of zone 2 suggest that river sediments were as equally important to basin development when zone 3 was laid down.

Based on core logging (Section 4.2.1), deposition of zones 1-3 (Fig.s 13-17) is known to have been mostly influenced by input of volcanic products into the basin, particularly zones 1 and 3. Therefore, elemental variations in zones 1 and 3 are mostly due to volcanic inputs into the basin while river inputs and fluctuations in water level within the basin were mostly dominant during deposition of zone 2. At this level of understanding, deciphering chemical composition of the volcanic products, which influenced deposition of zones 1 and 3 (Fig.s 13-17), will help to confirm whether the associated volcanism is linked to tectonic rifting or not. This will be done upon correlation to known compositions of volcanic products

that originated from tectonic events that influenced basins development within the East African Rift System (e.g. Boccaletti et al., 1999).

Pearce & Norry (1979) used a plot of Zr/Y against ZR to establishing sources of volcanic products whereby they observed an increase in Zr/Y ratio from island arc and mid-ocean ridge to within plate basalts. Similar interpretation was adopted by Hiscott & Gill (1992) when they assessed igneous origin of Oligocene to Quaternary volcaniclastic sands and sandstones from the Izu-Bonin arc by using major and trace element geochemistry. In this work, the relationship between Zr/Y and Zr values (Fig. 18) has been established qualitatively in which most of the values are plotting outside the island arc, mid-oceanic ridge (MORB) and within plate (WPB) basalts ranges of Pearce & Norry (1979) and Hiscott & Gill (1992). An understanding that their WPB values were delivered from the oceanic crust allowed us to link further increase in Zr/Y values beyond the WPB range of Pearce & Norry (1979) to continental basalts since the plotted elemental values were measured from continental rift successions in the Eyasi-Wembere sub-basin. This is interpretation is likely because the Miocene-Quaternary volcanism of the East African Rift System is reported to have been dominated by eruption of basaltic products (Boccaletti et al., 1999). Thousands of kilometers north of the study area, deformation and magmatism linked with the EARs is concentrated along a narrow zone where by Early Pleistocene and Pliocene volcanic products exist (Boccaletti et al., 1999).

5. Discussion

5.1. Elemental variations with depth in the Eyasi-Wembere basin

Despite the observed general trends in zones 1-3 implying major and possibly regional sediments supply system in a basin, these zones are also characterized by several peaks and troughs reflecting local influences in elemental distributions as well. An example of this is the variations of Fe content, which has been used to suggest major sources of sediments into the basin, either being volcanic or river inputs. However, Fe variations can be locally linked to degree of chemical weathering. Lower part of the Eyasi-Wembere stratigraphy contains chemically weathered fragments that are reddish-brown to light orange colored (Fig. 6). This part is interpreted to contain iron precipitates because of the Fe values that are locally high in all intervals that are reddish-brown to light orange colored. Despite the highlighted local fluctuations in elemental distributions, the observed general trends in zones 1-3 show that deposition of zones 1 and 3 was mostly influenced by input of volcanic products while river inputs were mostly dominant during deposition of zone 2.

There was no dateable fossils that could allow direct age assignment for zones 1 and 2 in the Eyasi-Wembere stratigraphy (Table 1). Biostratigraphy data (Table 1) has shown that the upper part of the cored deposits in the Eyasi-Wembere basin (zone 3 in Fig.s 13-17) is of Pleistocene-Holocene in age. Stratigraphically, this part conform to Pleistocene-Holocene syn-rift deposits and magmatic features on Fig.s 10-12 indicating that volcanism was linked to tectonic activities in the basin. Presence of volcanic

products in the lower part of the stratigraphy has allowed the Miocene-Pliocene tentative age to be assigned to zone 1 based on correlation with age equivalent tectonic features in the Tanga offshore basin. The fact that the cored volcanic products in the Eyasi-Wembere basin conform to features interpreted to indicate magmatic bodies in the Tanga offshore basin imply that these deposits are indeed existing in the Tanga offshore basin.

5.2. Tectonic events and occurrence of magmatic activities

The Miocene and Quaternary tectonic episodes are clearly manifested by remnant seismic rift features off the coast of Tanzania (Fig. 10). These tectonic episodes, which were identified based on wedge shaped fills indicative of syn-rift deposits (summarized by a cartoon shown on Fig. 19), conform to age equivalent intervals that contain volcaniclastic sediments in the Eyasi-Wembere basin. This correlation has allowed us to conclude that the volcanic inputs during the Miocene-Quaternary sedimentation of the Eyasi-Wembere basin were most likely delivered from the contemporaneous volcanism associated with the rifting and not from external vents or sources. This conclusion implies that the observed magmatic bodies in the Tanga offshore basin are due to contemporaneous volcanism associated with the East African Rift System in the offshore settings of Tanzania as their occurrences coincide with periods of active tectonics.

5.3. Petroleum potential

5.3.1. Petroleum system elements

The Tanga offshore basin contain syn-rift and post rift successions with possible clastic source and cap rocks and potential petroleum reservoirs. The revealed magmatic deposits may form good petroleum reservoirs in a basin (e.g. Chen et al., 1999). Possible traps include localized force folds (Fig. 20) and the Quaternary extensive fault system in the basin (Mvile et al., 2021; Fig. 10).

5.3.2. Presence of magmatic intrusions

The igneous dyke on Fig. 12 cuts across most of the Miocene-Quaternary stratigraphy of the study area. The crosscut intervals include rocks with reservoir potential (deposits with high reflection amplitude interpreted to be sandstone bodies) and possible source and cap rocks (weak amplitude-reflection free intervals interpreted to be hemipelagic shale deposits). Presence of magmatic intrusions may have both negative and positive impacts as far as the petroleum potential of the basin is taken into consideration (e.g. Chen et al., 1999; Kharin & Eroshenko, 2014; Planke et al., 2018). Magmatic intrusions are associated with high geothermal gradient that may facilitate early maturation of the organic-rich rocks for charging the reservoirs in the basin but may also lead to formation of fractured reservoirs, igneous seals and structural elements that permit petroleum accumulation (e.g. Chen et al., 1999; Muirhead et al., 2017; Planke et al., 2018; Spacapan et al., 2020). Further work will involve extensive mapping of the basin using all available 2D seismic data coupled with field potential data (gravity and magnetic) for a full understanding on the sizes, age, volumes, distribution, and assessment of thermal effects of the magmatic intrusions on the petroleum potential of the Tanga offshore basin. This is because apart from

enhancing petroleum prospectivity of the basin, the magmatic activities may also have negative consequences including overcooking of the source rock, thermal destruction of the already accumulated petroleum in the reservoir and reduction of reservoir porosity and permeability due to precipitation of the associated hydrothermal fluids (e.g. Chao et al., 2015; Planke et al., 2018). However, preliminary results suggest that thermal destruction of the accumulated hydrocarbons is less likely because the revealed intrusions occurred during periods of active tectonics that controlled syn-rift sedimentation, the time during which the organic-rich rocks and their associated reservoirs were laid down.

5.3.3. Potential reservoir, source and cap rocks

Lower parts of the syn-rift deposits in Fig. 10 contain seismic deposits with low seismic amplitude-transparent configuration. Deposits with similar seismic manifestation have been interpreted to indicate presence of hemipelagic mud/shale successions in several basins (e.g. Berlin, 2014; Fonnesu et al., 2020). Similar interpretation has been made made in this case. These hemipelagic shale successions are bounded by high amplitude reflectors implying episodic influx of fine-grained inputs alternating with high amplitude seismic reflections indicative of coarse sand deposits in the rift sub-basins bounded by major faults (Fig. 10). The sand and shale deposits in the Tanga offshore basin may be well sorted and more laterally extensive due to their furthest distance from the hinterland respectively. These properties may cause the former to be good reservoirs and the latter to have improved source rock properties and sealing capacities for petroleum accumulations. The coarse sand deposits onlapping onto the localized fold structures and their superjacent fine grained deposits (Fig. 19) may also form potential reservoirs and source and cap rocks respectively.

6. Conclusion

This study used the available 2D seismic lines to constrain timing of the Miocene-Quaternary tectonic events relative to occurrence of magmatic bodies in the Tanga offshore basin. Miocene-Holocene strata of the Tanga offshore basin are interpreted to have been intruded by magmatic bodies. These magmatic bodies have not been penetrated by wellbores and therefore their discovery was based on interpretation of 2D seismic data and correlation with age equivalent deposits in the Eyasi-Wembere basin. The proposed timing of magmatic intrusions in the Tanga offshore basin conform to proposed timing of emplacement of volcaniclastic deposits cored in the southwestern margin of the Eyasi-Wembere basin. The associated magmatism stages are linked to tectonic events within the East African Rift System and that the volcanic inputs during Miocene-Quaternary sedimentation originated from volcanism that occurred contemporaneously to rifting. Presence of these magmatic bodies in the Miocene-Quaternary stratigraphy has implications for petroleum potential in the Tanga offshore basin. The detailed 2D qualitative seismic interpretation has revealed presence of sedimentary systems with potential structural elements, reservoirs and source and cap rocks intervals for potential petroleum generation and trapping in the basin. Formation of some structural elements, including localized folds, and possible maturation of the source intervals in the basin are thought to have been facilitated by magmatic intrusions.

Declarations

Conflict of Interest

On behalf of all authors, the corresponding author states that there is no conflict of interest.

Acknowledgement

Pan African University Life and Earth Sciences Institute (PAULESI) is highly acknowledged for the award of PhD Scholarship to the first author. The University of Dodoma is well addressed for granting study leave to the first author. Accesses to the dataset used to accomplish this work were provided by Tanzania Petroleum Development Corporation (TPDC) and Tanzania Petroleum Upstream Regulatory Authority (PURA). The authors are thankful to the University of Dar es Salaam for allowing access to their facilities to be used for data analysis.

Funding: Not applicable

Conflicts of interest/Competing interests: Not applicable

Availability of data and material: Not applicable

Code availability: Not applicable

Authors' contributions: Not applicable

References

1. Algeo TJ, Maynard JB (2004) Trace-element behavior and redox facies in core shales of Upper Pennsylvanian Kansas-type cyclothems. Chem Geol 206(3–4):289–318
2. Armitage DA, McHargue T, Fildani A, Graham SA (2012) Postavulsion channel evolution: Niger Delta continental slopeNigeria Avulsions. AAPG Bull 96(5):823–843
3. Berlin TL (2014) Channel-levee complexes and sediment flux of the Upper Indus Fan. Master's Theses, LSU
4. Boccaletti M, Mazzuoli R, Bonini M, Trua T, Abebe B (1999) Plio-Quaternary volcanotectonic activity in the northern sector of the Main Ethiopian Rift: relationships with oblique rifting. J Afr Earth Sc 29(4):679–698
5. Brumsack HJ (2006) The trace metal content of recent organic carbon-rich sediments: implications for Cretaceous black shale formation. Palaeogeogr, Palaeoclimatol Palaeoecol 232(2–4):344–361
6. Calvert SE, Pedersen TF (1993) Geochemistry of recent oxic and anoxic marine sediments: implications for the geological record. Mar Geol 113(1–2):67–88

7. Chen Z, Yan H, Li J, Zhang G, Zhang Z, Liu B (1999) Relationship between Tertiary volcanic rocks and hydrocarbons in the Liaohe basin, People's Republic of China. AAPG Bull 83(6):1004–1014
8. Chorowicz J (2005) The east African rift system. J Afr Earth Sc 43(1–3):379–410
9. Courgeon S, Bachèlery P, Jouet G, Jorry SJ, Bou E, BouDagher-Fadel MK, Poli E (2018) The offshore east African rift system: new insights from the Sakalaves seamounts (Davie Ridge, SW Indian Ocean). Terra Nova 30(5):380–388
10. Dymond J, Collier R (1996) Particulate barium fluxes and their relationships to biological productivity. Deep Sea Res Part II 43(4–6):1283–1308
11. Ebinger C, Djomani YP, Mbede E, Foster A, Dawson JB (1997) Rifting archaean lithosphere: the eyasi-manyara-natron rifts, east africa. J Geol Soc 154(6):947–960
12. Eide CH, Schofield N, Lecomte I, Buckley SJ, Howell JA (2018) Seismic interpretation of sill complexes in sedimentary basins: implications for the sub-sill imaging problem. J Geol Soc 175(2):193–209
13. Elliott GM, Jackson CAL, Gawthorpe RL, Wilson P, Sharp IR, Michelsen L (2017) Late syn-rift evolution of the Vingleia Fault Complex, Halten Terrace, offshore Mid-Norway; a test of rift basin tectono-stratigraphic models. Basin Res 29:465–487
14. Franke D, Jokat W, Ladage S, Stollhofen H, Klimke J, Lutz R, Schreckenberger B (2015) The offshore East African Rift System: Structural framework at the toe of a juvenile rift. Tectonics 34(10):2086–2104
15. Fonnesu M, Palermo D, Galbiati M, Marchesini M, Bonamini E, Bendias D (2020) A new world-class deep-water play-type, deposited by the syndepositional interaction of turbidity flows and bottom currents: The giant Eocene Coral Field in northern Mozambique. Mar Pet Geol 111:179–201
16. Foster A, Ebinger C, Mbede E, Rex D (1997) Tectonic development of the northern Tanzanian sector of the East African rift system. Geological Society [London] Journal, p 154
17. Friis H, Poulsen MLK, Svendsen JB, Hamberg L (2007) Discrimination of density flow deposits using elemental geochemistry—implications for subtle provenance differentiation in a narrow submarine canyon, Palaeogene, Danish North Sea. Mar Pet Geol 24(4):221–235
18. Hansen DM, Redfern J, Federici F, Di Biase D, Bertozzi G (2008) Miocene igneous activity in the Northern Subbasin, offshore Senegal, NW Africa. Mar Pet Geol 25(1):1–15
19. Hiscott RN, Gill JB (1992) Major and trace element geochemistry of Oligocene to Quaternary volcaniclastic sands and sandstones from the Izu–Bonin Arc. In *Proceedings of the Ocean Drilling Program, Scientific Results* (Vol. 125, pp. 467-486). Government Printing Office College Station Texas
20. Kapilima S (2003) Tectonic and sedimentary evolution of the coastal basin of Tanzania during the Mesozoic times. Tanzania Journal of Science 29(1):1–16
21. Kent PE, Hunt JA, Johnstone DW (1971) The Geology and Geophysics of Coastal Tanzania. Institute of Geological Sciences Geophysical Paper No. 6

22. Kharin GS, Eroshenko DV (2014) Basic intrusives and hydrocarbonic potential of the South-East Baltic. Oceanology 54(2):245–258
23. Kiswaka EB, Felix M (2020) Permo-Triassic sedimentary fills and tectonic phases off Mid Norway: seismic investigation of the Trøndelag Platform.*Norwegian Journal of Geology/Norsk Geologisk Forening*, *100*(1)
24. Liu C, Xie Q, Wang G, Cui Y, Zhang C (2015) The influence of igneous intrusion to detrital reservoir: advances and outlook. Adv Earth Sci 30(6):654–667
25. Muirhead DK, Bowden SA, Parnell J, Schofield N (2017) Source rock maturation owing to igneous intrusion in rifted margin petroleum systems. J Geol Soc 174(6):979–987
26. Martinez-Ruiz F, Kastner M, Gallego-Torres D, Rodrigo-Gámiz M, Nieto-Moreno V, Ortega-Huertas M (2015) Paleoclimate and paleoceanography over the past 20,000 yr in the Mediterranean Sea Basins as indicated by sediment elemental proxies. Q Sci Rev 107:25–46
27. Martınez-Ruiz F, Paytan A, Kastner M, Gonzalez-Donoso JM, Linares D, Bernasconi SM, Jimenez-Espejo FJ (2003) A comparative study of the geochemical and mineralogical characteristics of the S1 sapropel in the western and eastern Mediterranean. Palaeogeogr, Palaeoclimatol Palaeoecol 190:23–37
28. Mbede EI (2001) Tectonic setting and uplift analysis of the Pangani rift basin in northern Tanzania using apatite fission track thermochronology. Tanzania Journal of Science 27(2):23–38
29. Mollel GF, Swisher III, C. C (2012) The Ngorongoro Volcanic Highland and its relationships to volcanic deposits at Olduvai Gorge and East African Rift volcanism. J Hum Evol 63(2):274–283
30. Müller R, Ngstuen JP, Eide F, Lie H (2005) Late Permian to Triassic basin infill history and palaeogeography of the Mid-Norwegian shelf—East Greenland region.. In Norwegian Petroleum Society Special Publications, vol 12. Elsevier, pp 165–189
31. Mvile BN, Kiswaka EB, Osinowo OO, Marobhe IM, Olayinka AI, Mshiu EE (2021) Cretaceous–Quaternary seismic stratigraphy of the Tanga offshore Basin in Tanzania and its petroleum potential.*Journal of Petroleum Exploration and Production Technology*,1–20
32. Nottvedt A, Gabrielsen RH, Steel RJ (1995) Tectonostratigraphy and sedimentary architecture of rift basins, with reference to the northern North Sea. Mar Pet Geol 12(8):881–901
33. Planke S, Rabbel O, Galland O, Millett JM, Manton B, Jerram DA, Spacapan JB (2018) Seismic imaging and petroleum implications of igneous intrusions in sedimentary basins constrained by outcrop analogues and seismic data from the Neuquen Basin and the NE Atlantic. In *10o CONGRESO DE EXPLORACIÓN Y DESARROLLO DE HIDROCARBUROS*
34. Pearce JA, Norry MJ (1979) Petrogenetic implications of Ti, Zr, Y, and Nb variations in volcanic rocks. Contrib Miner Petrol 69(1):33–47
35. Poulsen MLK, Friis H, Svendsen JB, Jensen CB, Bruhn R (2007) The application of bulk rock geochemistry to reveal heavy mineral sorting and flow units in thick, massive gravity flow deposits, Siri Canyon Palaeocene sandstones, Danish North Sea. Dev Sedimentol 58:1099–1121

36. Prosser S (1993) Rift-related linked depositional systems and their seismic expression. Geological Society, London, Special Publications 71(1):35–66
37. Ragon T, Nutz A, Schuster M, Ghienne JF, Ruffet G, Rubino JL (2019) Evolution of the northern Turkana Depression (East African Rift System, Kenya) during the Cenozoic rifting: New insights from the Ekitale Basin (28-25.5 Ma). Geol J 54(6):3468–3488
38. Ravnås R, Bondevik K (1997) Architecture and controls on Bathonian–Kimmeridgian shallow-marine synrift wedges of the Oseberg–Brage area, northern North Sea. Basin Res 9(3):197–226
39. Sakai T, Saneyoshi M, Sawada Y, Nakatsukasa M, Kunimatsu Y, Mbua E (2013) Early continental rift basin stratigraphy, depositional facies and tectonics in volcaniclastic system: examples from the Miocene successions along the Japan Sea and in the East African Rift Valley (Kenya). *Mechanism of Sedimentary Basin Formation—Multidisciplinary Approach on Active Plate Margins. InTech, Rijeka*, 83-108
40. Sangiorgi F, Dinelli E, Maffioli P, Capotondi L, Giunta S, Morigi C, Corselli C (2006) Geochemical and micropaleontological characterisation of a Mediterranean sapropel S5: a case study from core BAN89GC09 (south of Crete). Palaeogeogr, Palaeoclimatol Palaeoecol 235(1–3):192–207
41. Schoepfer SD, Shen J, Wei H, Tyson RV, Ingall E, Algeo TJ (2015) Total organic carbon, organic phosphorus, and biogenic barium fluxes as proxies for paleomarine productivity. Earth Sci Rev 149:23–52
42. Scholz CA, Rosendahl BR, Scott DL (1990) Development of coarse-grained facies in lacustrine rift basins: Examples from East Africa. Geology 18(2):140–144
43. Spacapan JB, Ruiz R, Manceda R, D'Odorico A, Rocha E, Vera ER, Galland O (2020) Oil production from a sill complex within the Vaca Muerta Formation
44. Ravnås R, Steel RJ (1998) Architecture of marine rift-basin successions. AAPG Bull 82(1):110–146
45. Tribovillard N, Algeo TJ, Lyons T, Riboulleau A (2006) Trace metals as paleoredox and paleoproductivity proxies: an update. Chem Geol 232(1–2):12–32
46. Trude KJ (2004) Kinematic indicators for shallow level igneous intrusions from 3D seismic data: evidence of flow firection and feeder location. Geological Society, London, Memoirs 29(1):209–218
47. Wehausen R, Brumsack HJ (1999) Cyclic variations in the chemical composition of eastern Mediterranean Pliocene sediments: a key for understanding sapropel formation. Mar Geol 153(1–4):161–176
48. Zhao F, Wu S, Sun Q, Huuse M, Li W, Wang Z (2014) Submarine volcanic mounds in the Pearl River mouth basin, northern South China Sea. Mar Geol 355:162–172
49. Zhao Y, Tong D, Song Y, Yang L, Huang C (2016) Seismic reflection characteristics and evolution of intrusions in the Qiongdongnan Basin: Implications for the rifting of the South China Sea. J Earth Sci 27(4):642–653

Figures

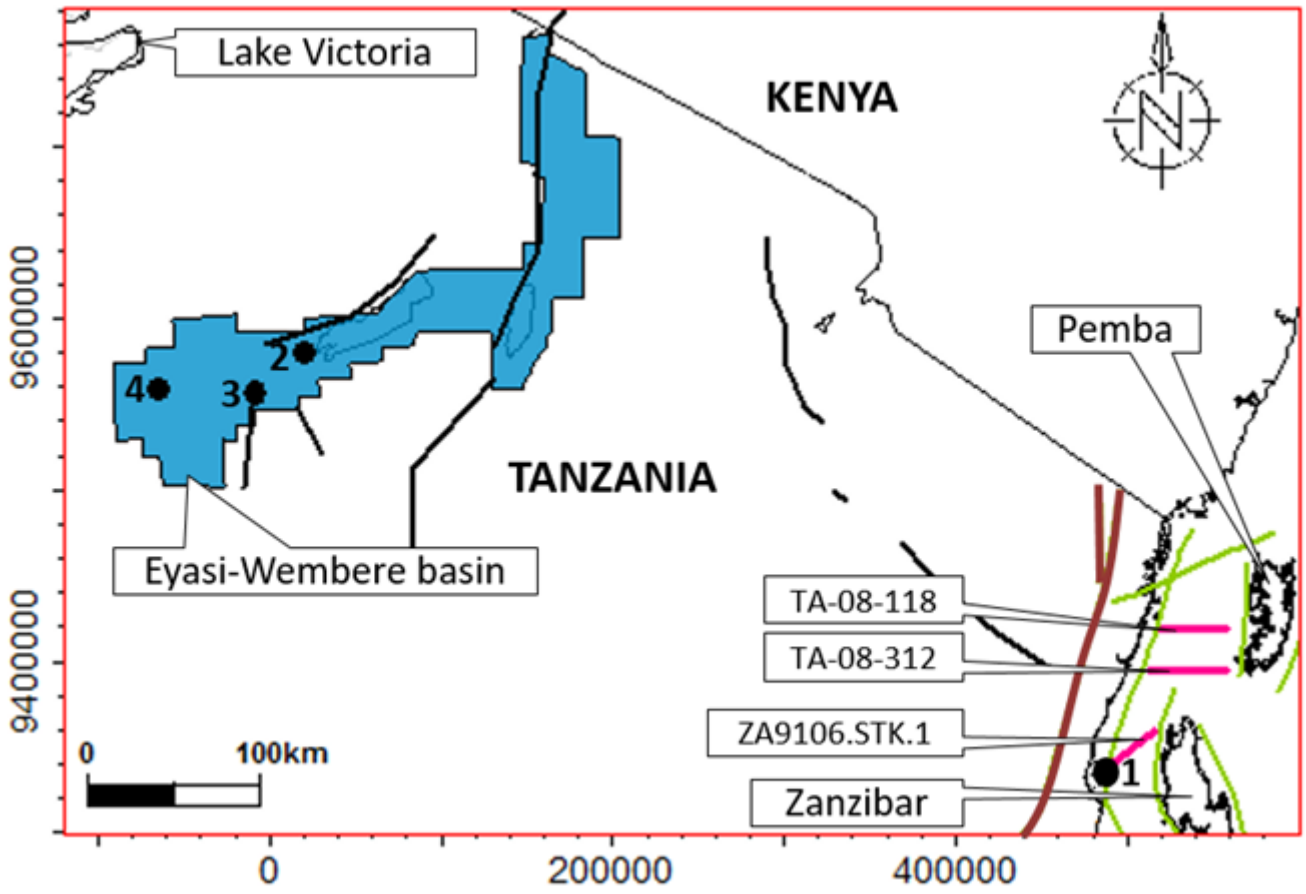

Figure 1

Map of the study area showing locations of the Tanga offshore basin and the Eyasi-Wembere basin. Numbers 1-4 show locations of key wells (1 = Ras Machuisi North 1, 2= Wembere-1, 3= Wembere-2 and 4 = Wembere-3). Pink lines show locations of seismic profiles used in this work. Stuctural elements have been modified after Ebinger et al. (1997), Foster et al. (1997) and Kapilima (2003).

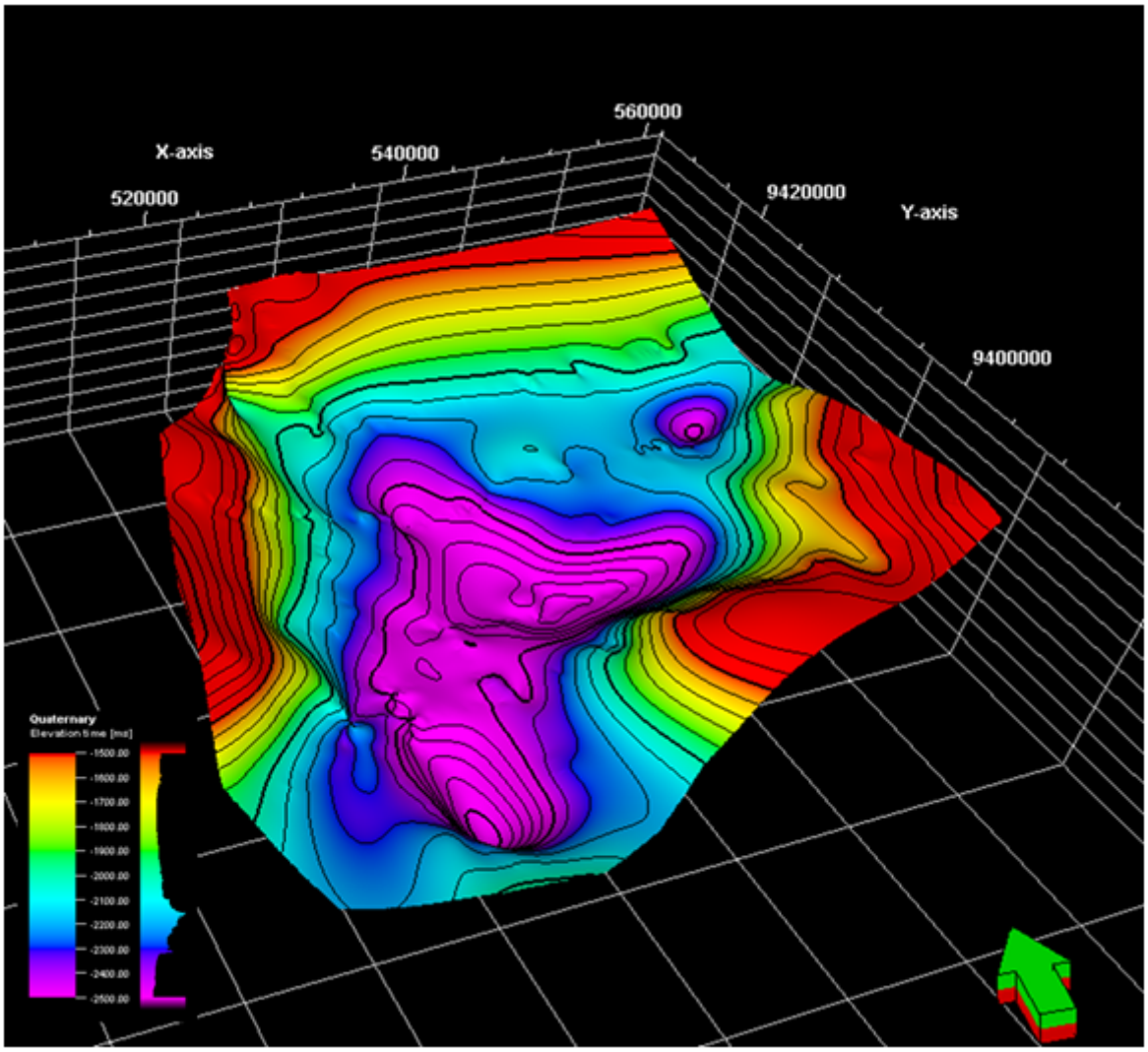

Figure 2

Base Quaternary surface map showing a N-S to NE-SW trending Quaternary sub-basin in the Tanga offshore basin. The sub-basin is bounded by major faults with NW, S-SE, E and N-NE dipping directions.

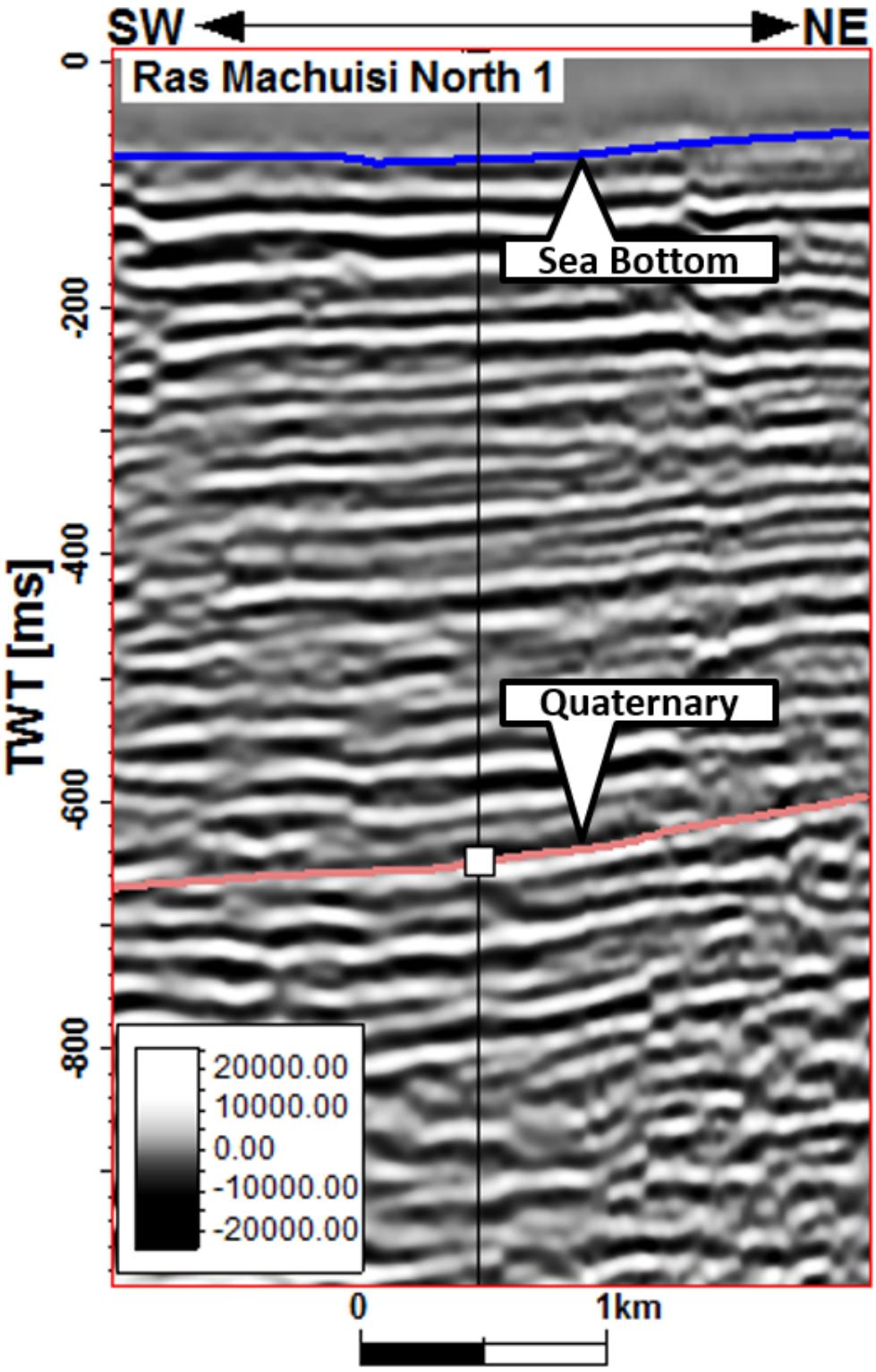

Figure 3

Part of seismic line ZA9106.STK.1 showing location of Ras Machuisi North 1 wellbore used to assign age to the studied seismic interval.

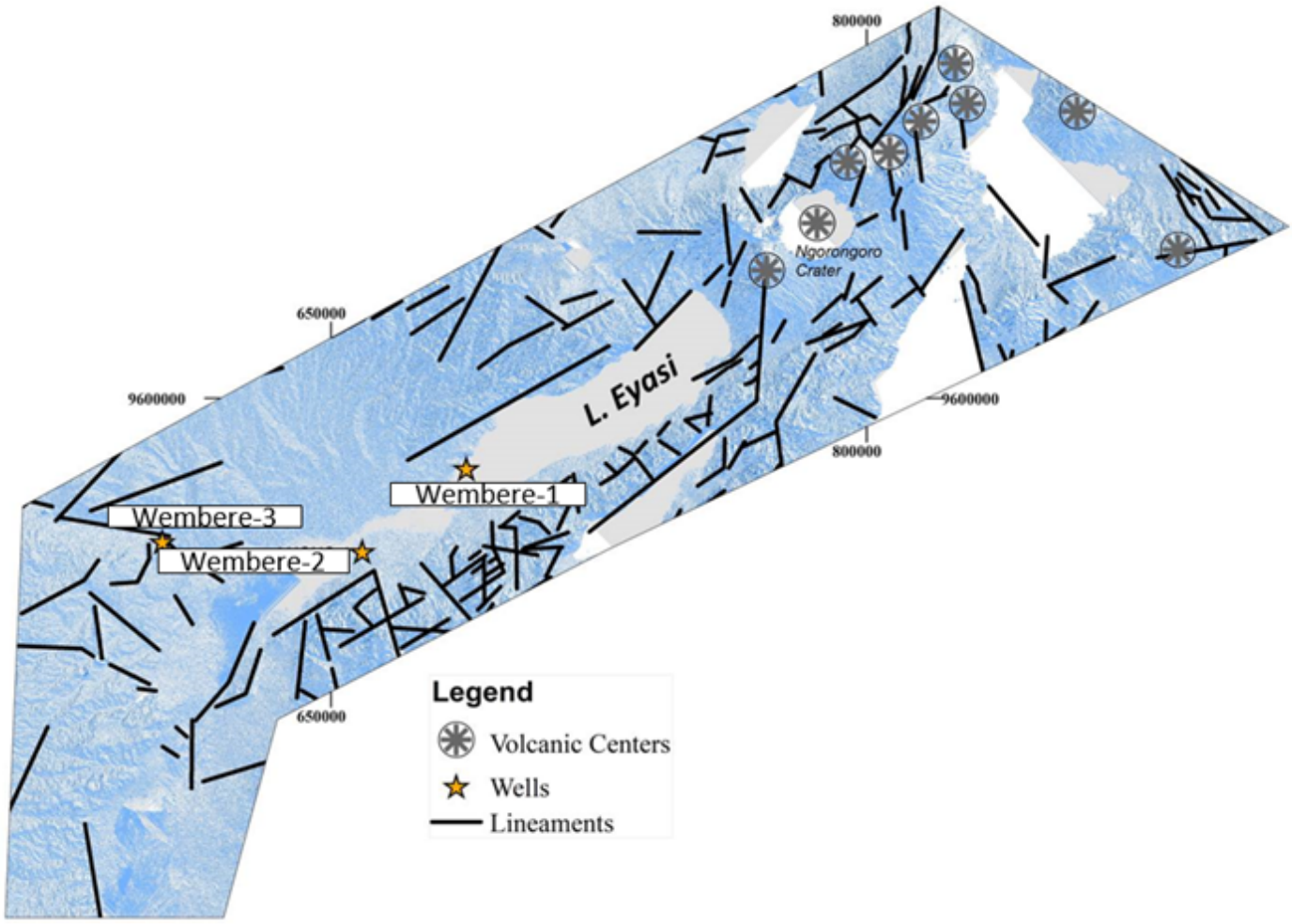

Figure 4

Structural elements map showing location of the Eyasi-Wembere basin relative to the volcanic centers (which are grouped as Ngorongoro volcanic centers for this study). Locations of the Wembere cores which were logged for establishment of the Eyasi-Wembere stratigraphy are also shown on this map.

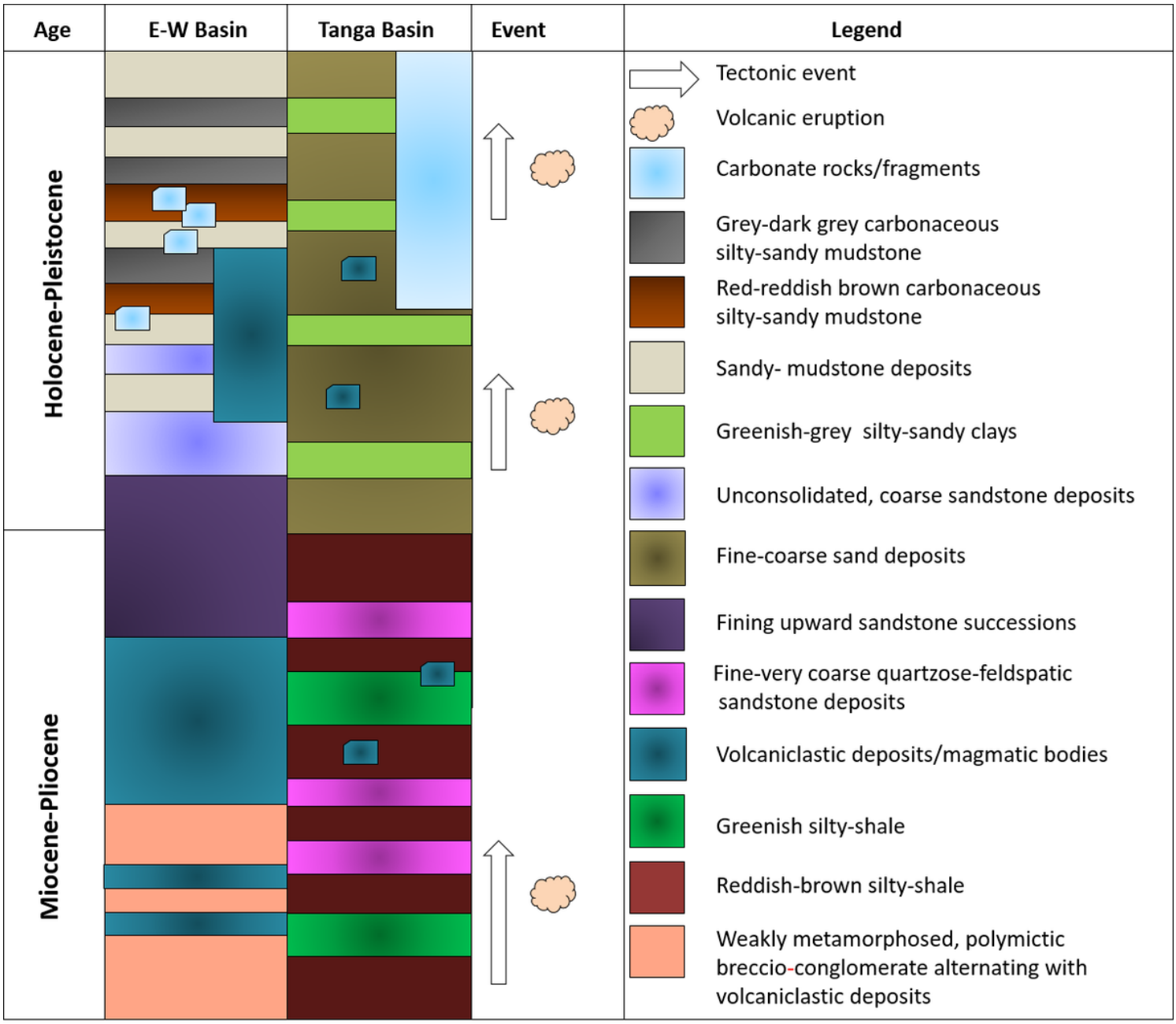

Figure 5

Correlated chronostratigraphic schemes between the Eyasi-Wembere and Tanga offshore basins with vertical positions of volcanic products and timing of tectonic events relative to volcanic eruptions/magmatic intrusions (see main text for description). E-W = Eyasi-Wembere.

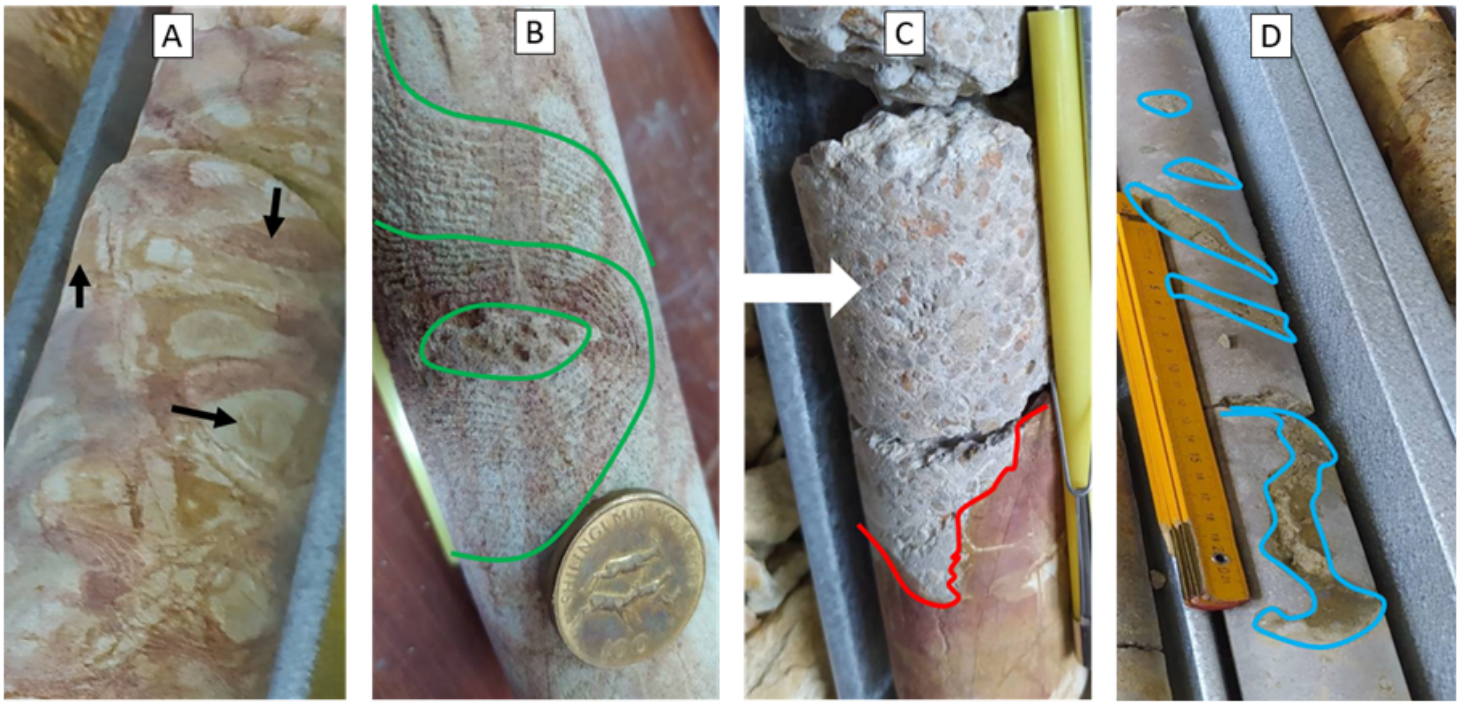

Figure 6

The Eyasi-Wembere core photos showing lower part of the penetrated intervals in the Eyasi-Wembere stratigraphy. A– polymictic breccio-conglomerates deposits. Black arrows on 'A' shows different sandstone fragments that have been chemically altered to different levels, and that is why they have different colors. B– complex fold and eye shaped structure (marked by green line) within a sandstone fragment. C– Red irregular line mark the boundary between conglomeratic sandstone deposits shown on 'A' and grain supported lapillistone (white arrow), volcaniclastic deposits characterizing lower part of the Eyasi-Wembere stratigraphy. D– volcanic ashes marked by blue closed lines within clastic deposits.

Figure 7

Poorly sorted, very coarse-conglomeratic sandstone deposits retrieved from the Wembere cores. A– close up view image showing poorly sorting nature of the deposits (purple arrow shows quartz grain while red arrow shows feldspar grain). B– core sample whereby fining upward pattern is seen (orange arrow shows the fining upward pattern in the sample).

Figure 8

Core photos showing sedimentary successions characterizing upper part of the Eyasi-Wembere stratigraphy. A– limestone fragment (demarcated by solid orange line) within grey, sandy-mudstone deposits in the lower section of the upper part of the stratigraphy. B– reddish silty-mudstone, C– grey carbonaceous silty-sandy mudstone, and D– dark grey mudstone deposits.

Figure 9

Paleogene-Neogene limestone exposure along the Tanga beaches. Notebook is used for scale purpose.

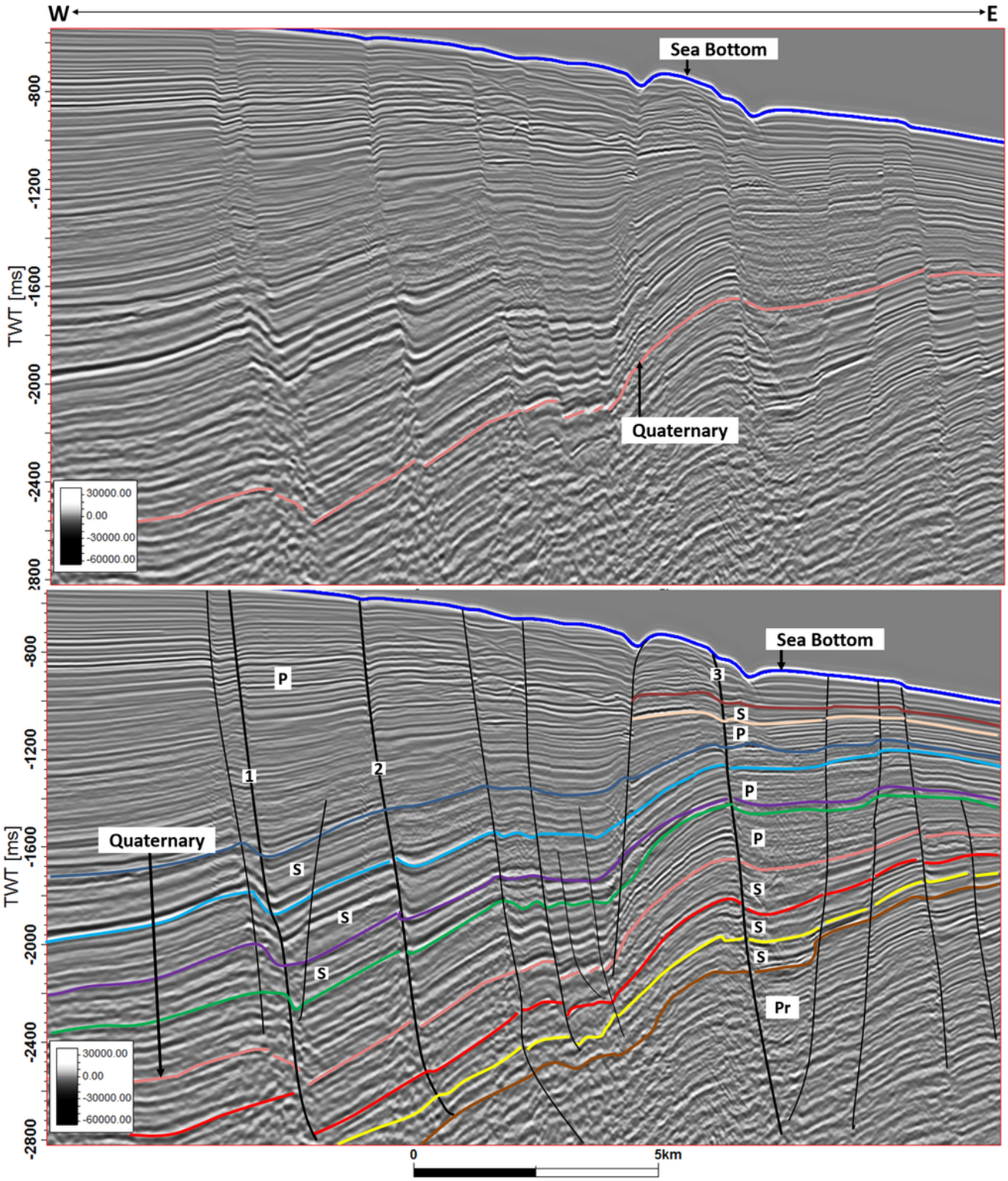

Figure 10

Seismic line TA-08-312 showing tectonic fearures in the Tanga offshore basin. Faults labeled 1-3 were chosen to show syn-rift sedimentation and timing of faults movement. Pr = pre-rift sedimentation, S = sedimentary wedges indicative of syn-rift sedimentation, P = post-rift sedimentation.

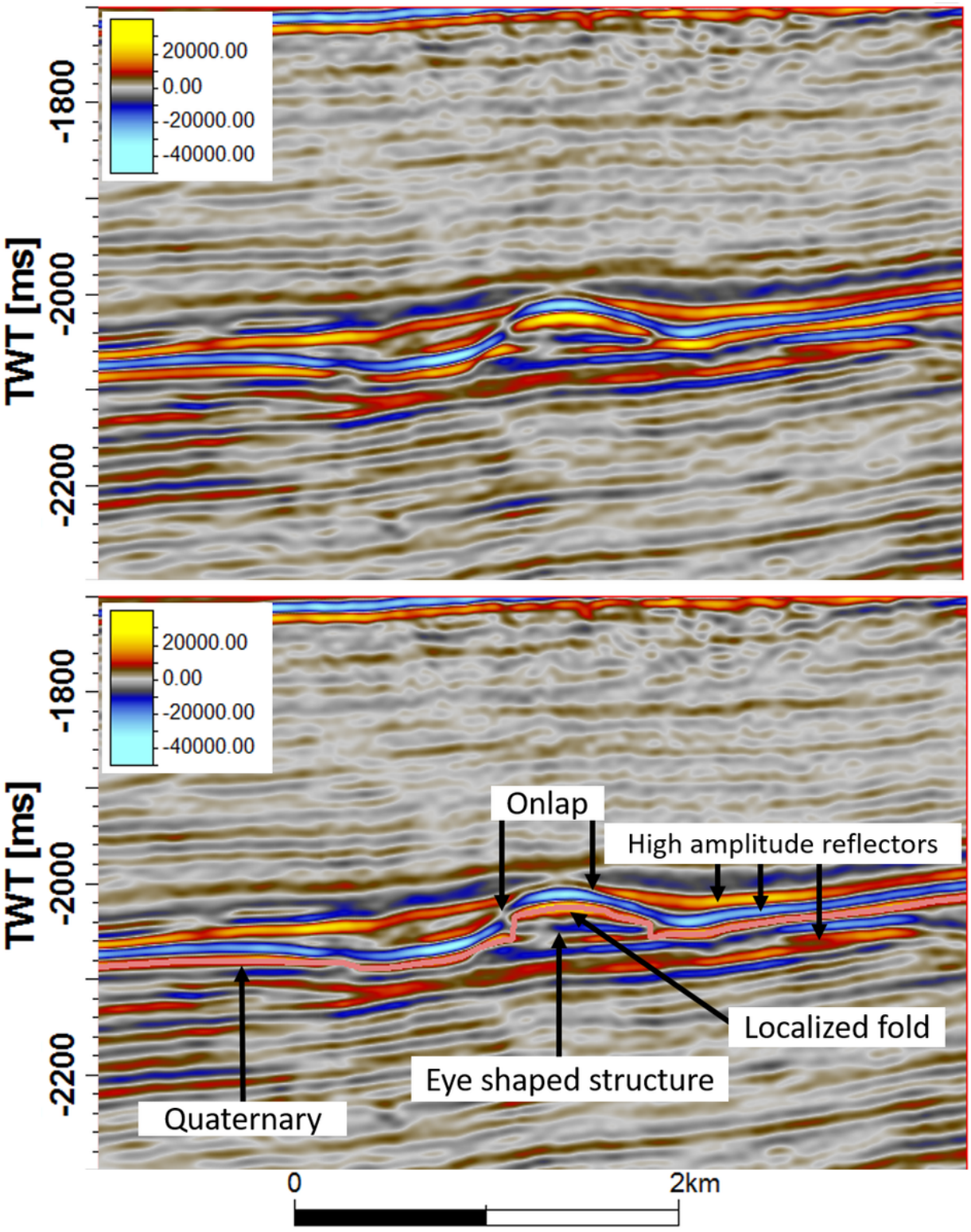

Figure 11

Part of seismic line TA-08-118 showing eye-shaped structure just at the Paleogene-Quaternary boundary. Other reflectors are onlapping onto the flanks of the eye-shaped structure.

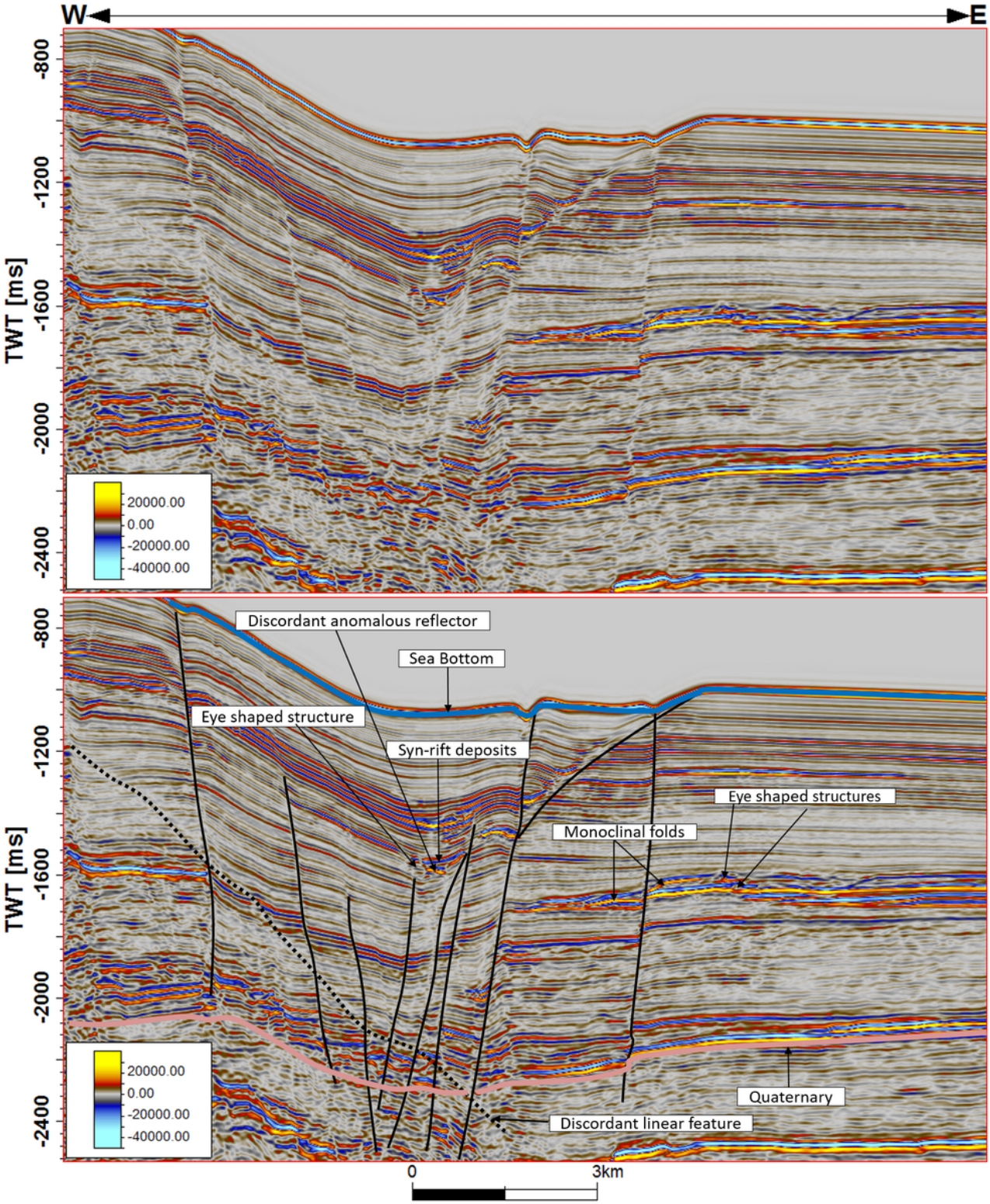

Figure 12

Uninterpreted and interpreted seismic line TA-08-118 showing tectonic and magmatic features in the Tanga offshore basin.

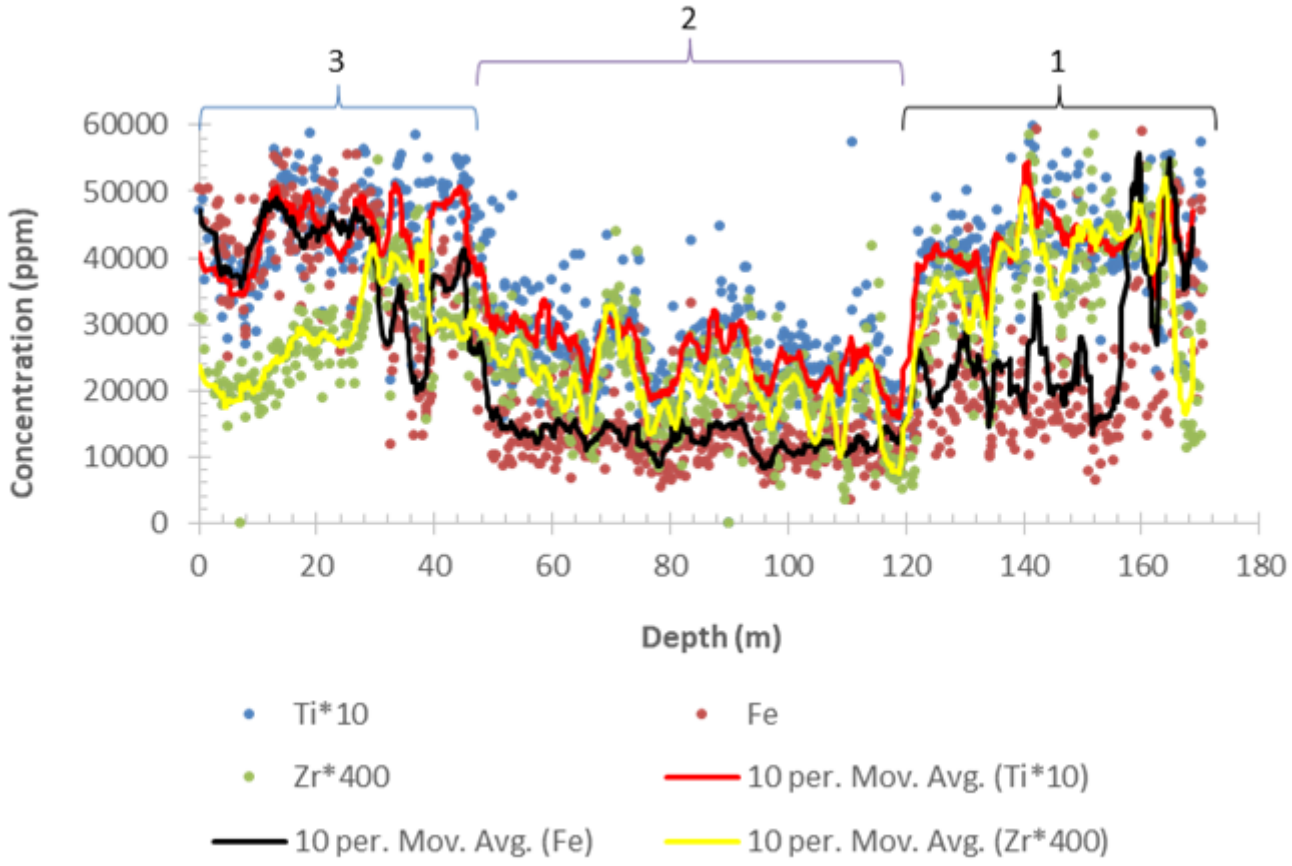

Figure 13

Distributions of Ti, Zr and Fe values (ppm) in the Wembere-3 core.

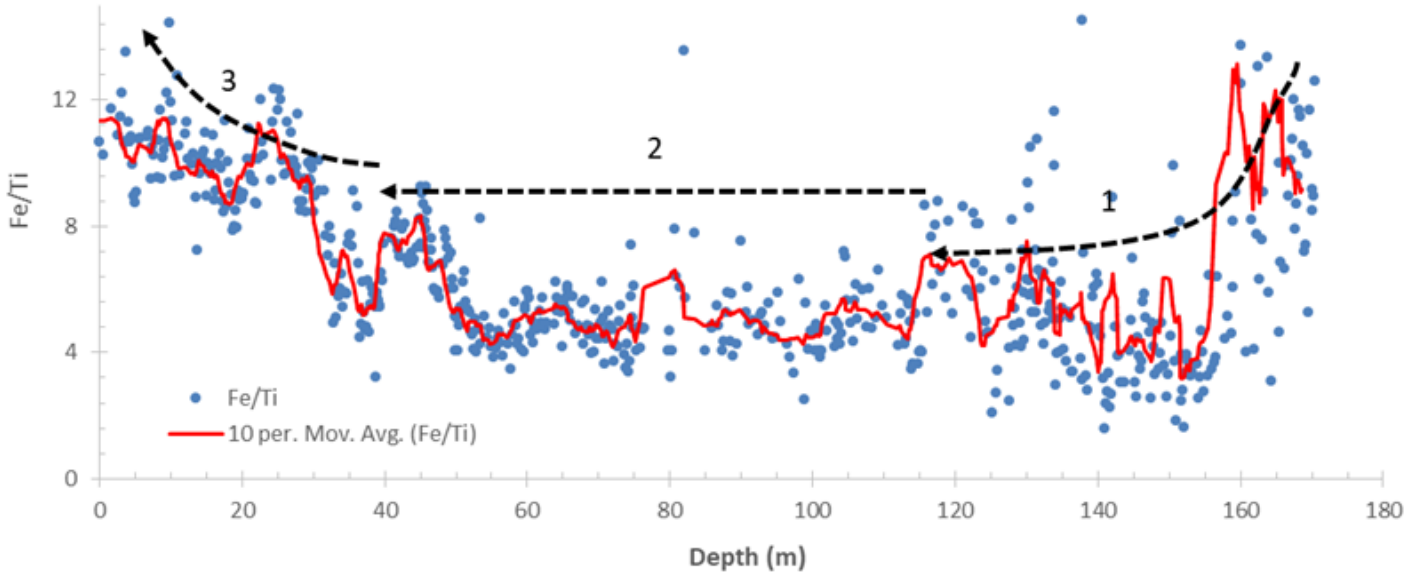

Figure 14

Plot of Fe/Ti versus depth in the Wembere-3 core. Arrows show Fe/Ti interpreted distribution trends in zones 1-3.

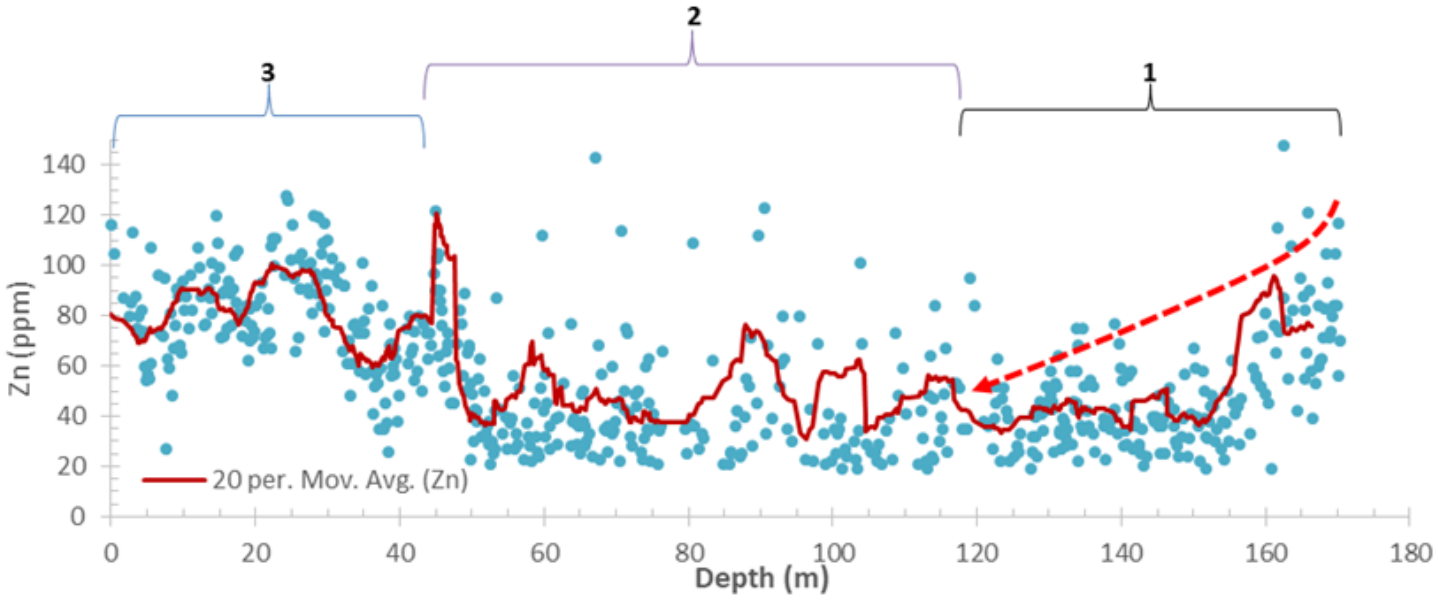

Figure 15

Zn (ppm) vertical distribution in the Wembere-3 core.

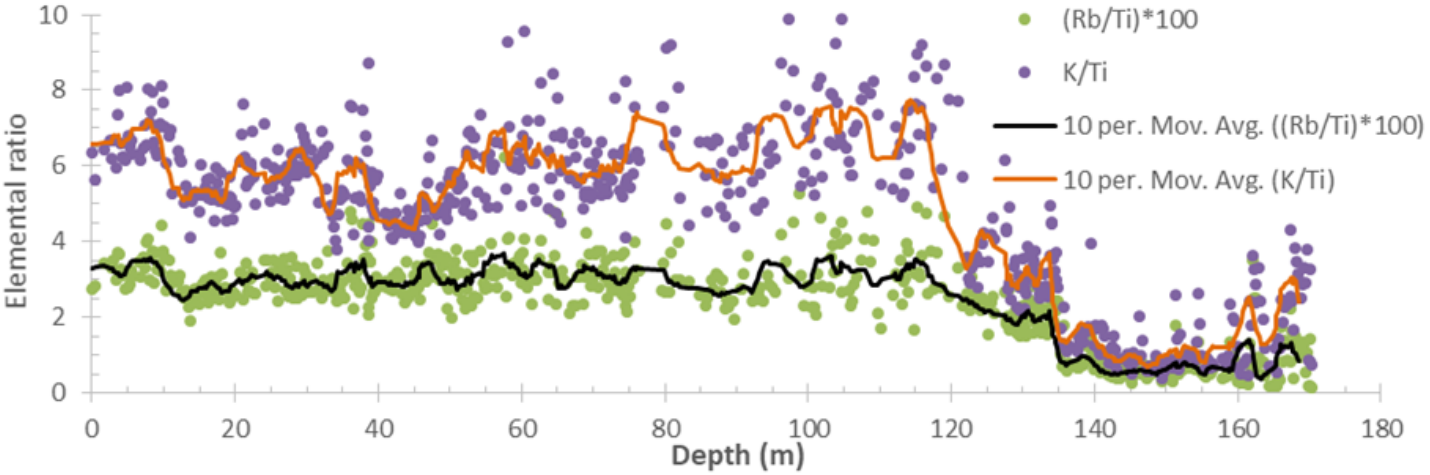

Figure 16

K/Ti and Rb/Ti values plotted against depth in the Wembere-3 core.

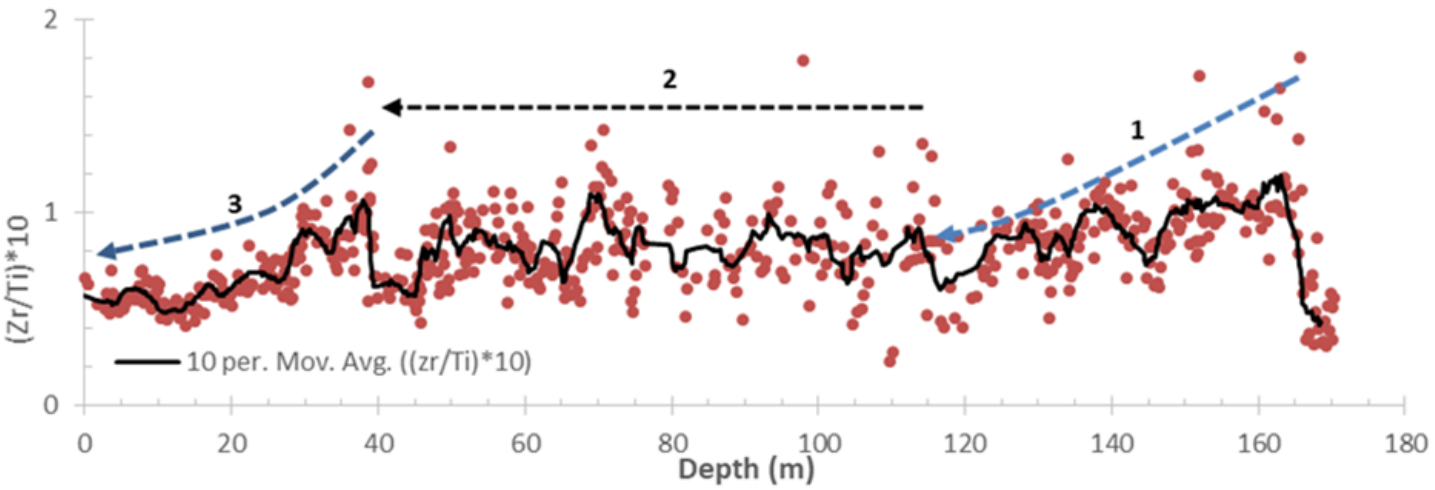

Figure 17

Zr/Ti values ploted against depth in the Wembere-3 core. Arrows show Zr/Ti interpreted distribution trends in zones 1-3.

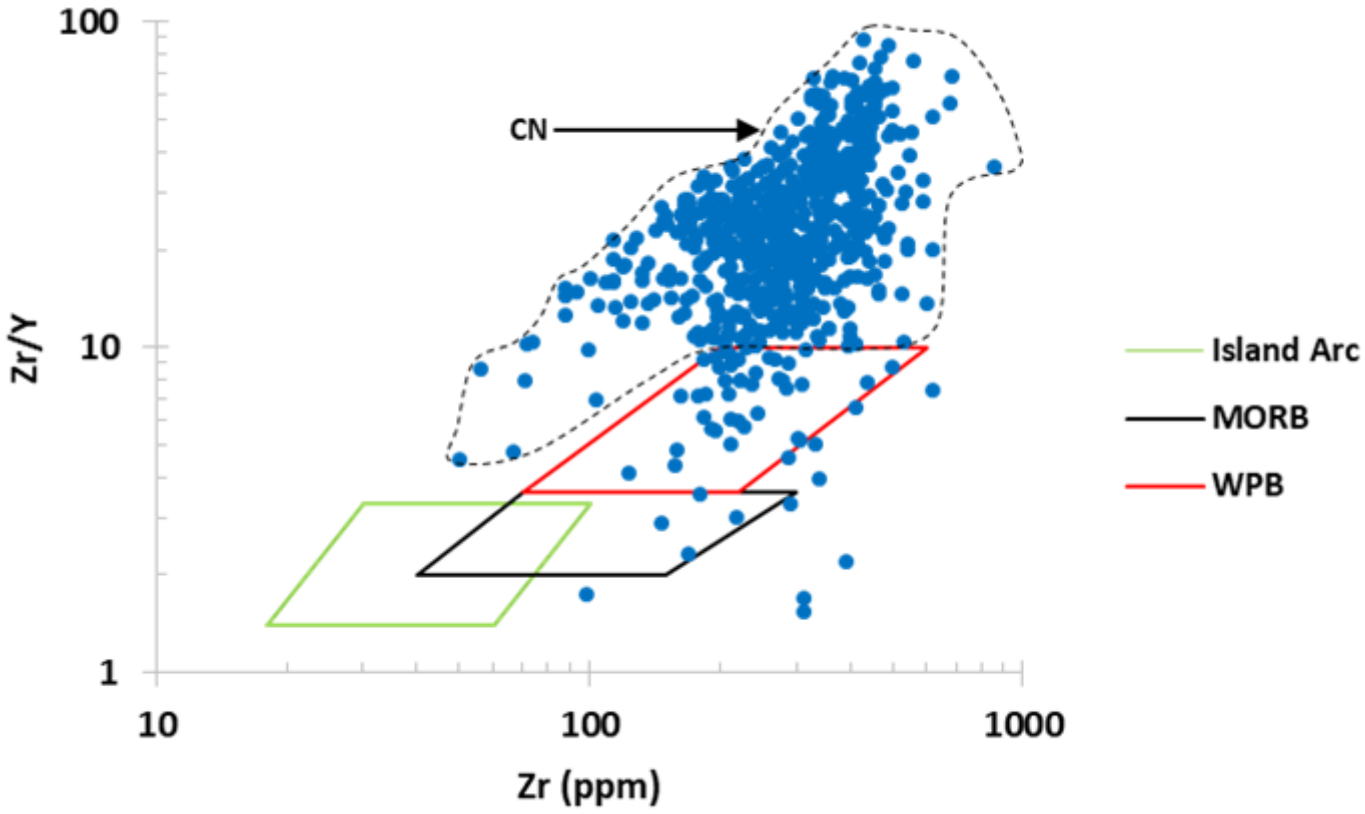

Figure 18

A plot of Zr/Y against ZR used to identify origin of the volcanic products in the Eyasi-Wembere sedimentary successions. CN – continental rift basalt.

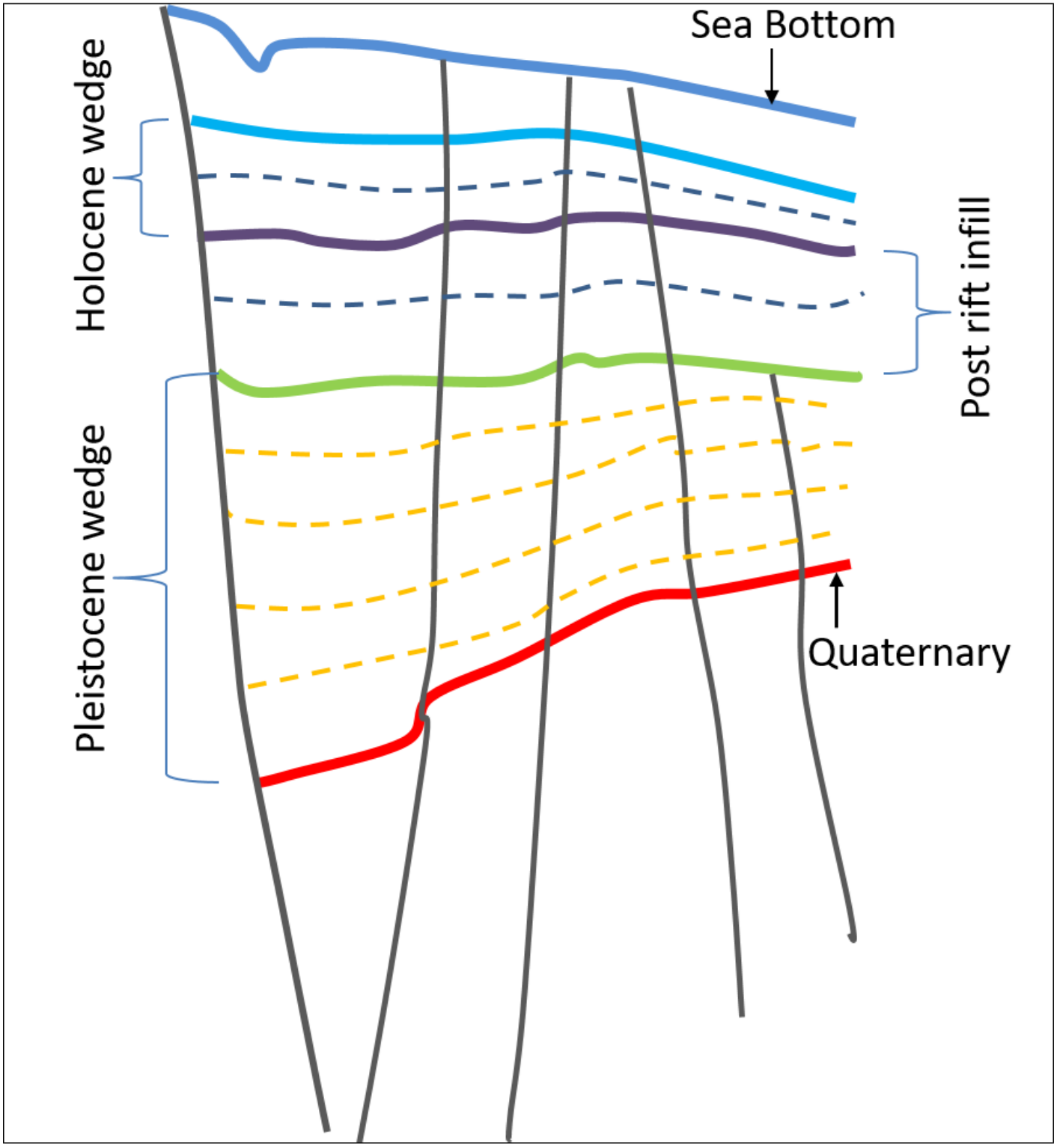

Figure 19

A cartoon summarizing Quaternary depositional geometries from Fig. 10. The Pleistocene and Holocene wedges indicative of syn-rift sedimentation are separated by a post-rift infill signifying intervening period of tectonic quiescence.

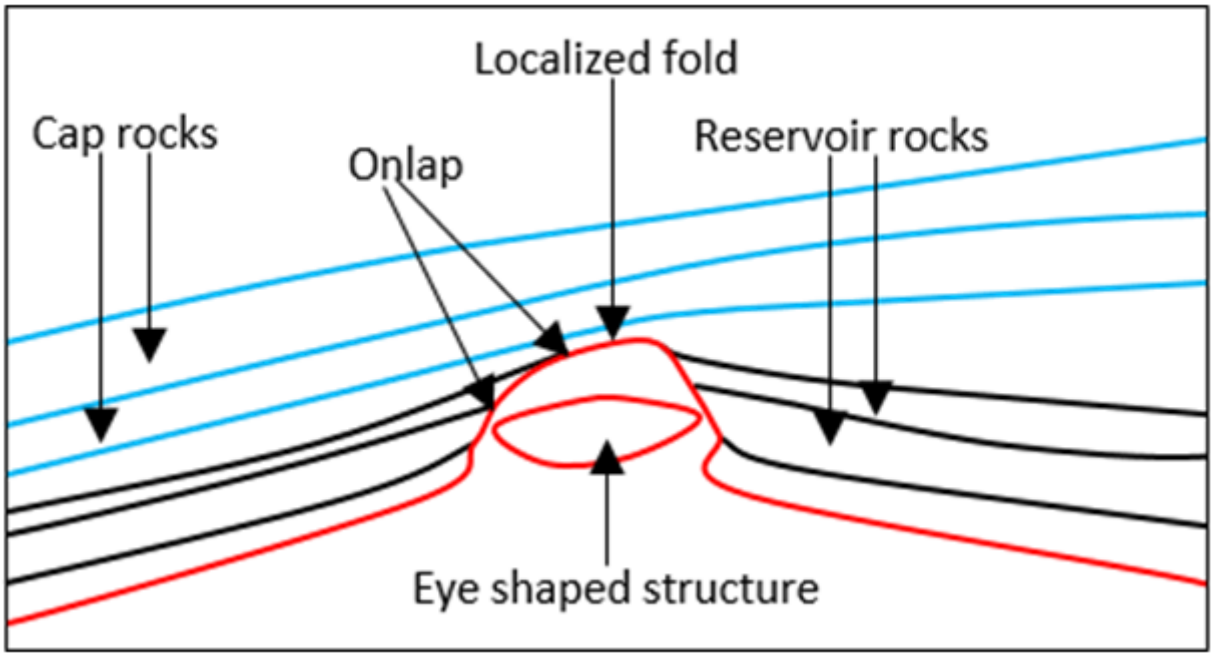

Figure 20

A cartoon illustrating potential petroleum system elements in the study area. Here a localized fold is interpreted to have resulted from magmatic intrusion indicated by the eye-shaped structure.